ABSTRACT

Title of Dissertation: MECHANISM OF DREAM COMPONENT *TSO1* IN PLANT STEM CELL REGULATION

Fuxi Wang, Doctor of Philosophy, 2022

Dissertation directed by: Professor Zhongchi Liu, CBMG

Plants are important for human survival and the environment. They provide oxygen, food, medicine and fuel. Understanding the development of plants has been a fundamental research question. Among all the plant tissues, the most important ones are the meristems. Sitting at the tip of the shoot and the root are the shoot apical meristem (SAM) and the root apical meristem (RAM). The shoot apical meristem gives rise to the above-ground organs like leaves and flowers while the root apical meristem produces all the root tissues that help to anchor the plants and transport water and nutrients. As the meristem is capable of producing new organs throughout the lifespan of a plant, the study of meristem maintenance and development provides the key to the understanding of plant development.

Arabidopsis transcription factor *TSO1* plays an essential role for the proper development of shoot apical meristem and root apical meristem. *TSO1* encodes a protein with a cysteine-rich repeats domain and TSO1 is a potential component of a cell cycle regulating complex, the DREAM complex. The *tso1-1* mutant has fasciated SAM due to shoot meristem cell over-proliferation and complete sterility due to lack of differentiated female and male floral organs. Interestingly, the *tso1-1* mutant also produces shorter root than the wild type, presumably caused by early

differentiation of the cells in the RAM. A prior mutagenesis screen identified two major suppressors of *tso1-1*. Characterization of these *tso1-1* suppressor mutations provides important insights to the understanding of TSO1-regulatory pathways. My dissertation project focuses on analyzing one of these suppressors that was shown to be a mutated type-A cyclin gene named *CYCA3;4*. Mutations in *CYCA3;4* suppress the shoot phenotype but not the root phenotype of *tso1-1*. The suppressed plants can produce normal floral organs and become partially fertile. Using transgenic method, I showed that the expression of *CYCA3;4* was increased in the *tso1-1* SAM, and overexpression of *CYCA3;4* in the *tso1-3* mutant enhanced the fertility defect, suggesting that overexpression of *CYCA3;4* partially mediates the *tso1-1* shoot phenotype. In addition, I provided evidence supporting that *TSO1* likely represses *CYCA3;4* gene expression indirectly through *MYB3R1*, whose mutations also suppress *tso1-1* mutants. My dissertation provides an important link between TSO1, a potential cell cycle regulatory complex component and meristem regulator, and cyclin A, a protein directly involved in cell cycle regulation. This link provides an important mechanistic insight into how plant meristems maintain their identity by limiting their cell division activity.

To further investigate the mechanism of *TSO1* action in the root, I collaborated with two other scientists to profile the gene expression in the *tso1-1* root at single cell level. I compared the single cell RNA sequencing data of *tso1-1* and wild type roots and identified molecular defects in the *tso1-1* root vasculature. Correspondingly, the known regulators of vasculature development, the *HD-ZIP III* genes, are ectopically expressed in some of the vascular cells in the *tso1-1* root. It suggests that the defects of root vasculature may be attributed to mis-expressed *HD-ZIP III* genes in the *tso1-1* mutant. The HD-ZIPIII function was previously linked to their regulation of cytokinin biosynthesis genes, which were ectopically expressed in *tso1-1* roots as

revealed by our scRNA-seq data. Together, our data suggest that the over-production of cytokinin might be the cause of *tso1-1* short root phenotype.

In summary, my dissertation research revealed previously unknown links between TSO1 and cell cycle regulation in the shoot and root meristems as well as the molecular mechanisms of *TSO1* function in the root vascular development at single cell level. These findings have furthered our understanding of how cell cycle regulation is integrated with plant development.

MECHANISM OF DREAM COMPONENT *TSO1* IN PLANT STEM CELL REGULATION

by

Fuxi Wang

Dissertation submitted to the Faculty of the Graduate School of the
University of Maryland, College Park, in partial fulfillment
of the requirements for the degree of
Doctor of Philosophy
2022

Advisory Committee:
Professor Zhongchi Liu, Chair
Associate Professor Stephen Mount
Associate Professor Antony Jose
Associate Professor Jianhua Zhu
Associate Professor Yiping Qi

Acknowledgements

I would like to thank my advisor Dr. Zhongchi Liu for her advice on experiments, critical thinking and writing over the past few years. She has been very patient and encouraging. She has confidence in me even sometimes I don't have that in myself. I can't be more grateful for the support she gave me: both the support on research and the support when I had hard times in my life. I see her as my role model as a scientist, especially as a female scientist.

I also want to thank my committee members. I bothered Dr. Steve Mount a lot with my questions. He has been a great help for me on research and how to deal with Covid situation. I enjoyed the afternoon teatime when we talked about science and shared the mooncakes. I benefit a lot from Dr. Antony Jose's writing class and continue to apply what I learned to my scientific writing, like this dissertation. Dr. Yiping Qi and Dr. Jianhua Zhu have been very supportive to my project and always make sure that I have a feasible plan for it.

I would like to acknowledge my collaborators Dr. Rachel Shahan in Dr. Philip Benfey's lab and Muzi Li in the Liu lab. They made the single cell project possible. It was difficult to perform the single cell sequencing during the pandemic, but Rachel did it! Muzi is a very good friend of mine. I am grateful not only for the work she has done but also her company when I had to work late.

I am so glad that I joined the Liu lab for my PhD study. Everyone I met in the Liu lab are so nice and caring. We talk about each other's project a lot and we are always happy to help each other with troubleshooting. I enjoyed a lot of our annual spring

trips and crab feast/fall hiking. I am also very grateful for the former lab members, especially Dr. Julie Caruana, Dr. Wanpeng Wang (George) and Dr. Junhui Zhou. Julie was one of the few people with whom I could share all my 'nerdy' stories. George has worked on the *TSO1* project before me. All my work wouldn't be possible without his solid groundwork. Junhui has been a great teacher on how to perform experiments. Whenever I had questions about any type of experiment, I always went to him, and I always got helpful suggestions. I also want to thank the undergraduate students who I had work with. They are Nicole Szeluga, Merixia Kunjal and Emmanuel Mgboji.

I am thankful for my friends outside the Liu lab too. Custódio Nunes and Matthew Fischer joined BISI the same year as me. We have been very good friends since then. We supported each other throughout the PhD study. Bilian Qian, Bixuan Wang and Jiming Wu also gave me a lot of support, especially during the pandemic. I also would like to thank my writing friend, Xiaojing Mao, who always encouraged me to write better and faster. I also would like to thank my idol Seventeen. Their music and stories have encouraged me to go further.

I would like to acknowledge the Dean's fellowship and the Ann G. Wylie dissertation fellowship.

I am grateful for the support from my boyfriend, Anxin Bai. He makes me feel like home when he is around.

Finally, I want to thank my families. My uncle has been taking good care of me since I arrived in Maryland. My parents have been incredibly supportive for every decision

I made. They gave me unconditional love and trust. I could not go this far without them.

Table of Contents

Chapter 1: Introduction

1.1 Plant meristem: origin of plant organs

1.1.1 Shoot apical meristem (SAM): structure and how it is maintained

One of the amazing facts about plants is that they continue to produce new organs throughout their lifetime, no matter it is a few weeks or hundreds of years. This is made possible by maintaining a small pool of pluripotent cells called the meristem. Similar to the stem cell in animals, the stem cells in plant meristem have the ability to maintain pluripotent state, continuously self-renewing and giving rise to daughter cells that form new plant organs. Different from animals, the fate of each plant cell is determined by its position relative to other cells rather than by the cell lineage as in most of the animals (Poethig, 1989).

There are three important meristems in plants: the shoot apical meristem (SAM), root apical meristem (RAM), and the vascular meristem (De Rybel *et al.*, 2016). The SAM gives rise to the above-ground tissues, the RAM produces cells to form the root, while the vascular meristem generates vascular tissues like xylem and phloem. This dissertation will focus on understanding the development of SAM and RAM.

The dome shaped *Arabidopsis* shoot apical meristem (SAM) consists of three functional domains: the stem cell bearing central zone (CZ), the rapidly dividing peripheral zone (PZ), and the rib zone (RZ) that provides new cells to form the internal tissues like the vasculature (Figure1.1 A and B). Sitting at the top of the RZ is a small group of cells named organizing center (OC), where a homeodomain

transcription factor named *WUSCHEL* (*WUS*) is expressed. *WUS* plays a vital role in maintaining the stem cells in *Arabidopsis* SAM: the *wus* mutants

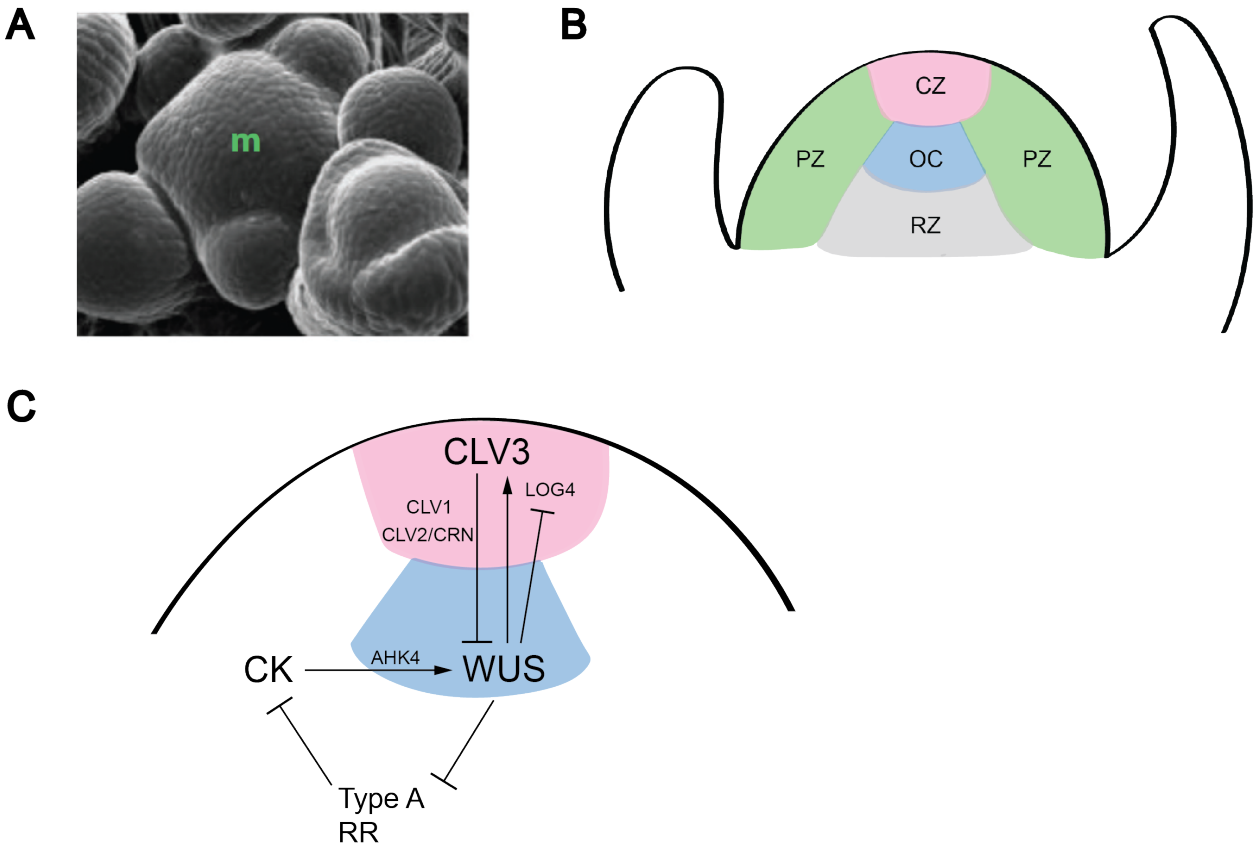

Figure 1.1: The structure of *Arabidopsis* SAM and the regulatory pathways for maintaining it.
(A) *Arabidopsis* shoot apical meristem under a scanning electron microscope. m =? (B) A diagram illustrating different domains within the SAM. CZ: central zone (pink), OC: organizing center (blue), PZ: prepherial zone (green), RZ: rib zone (gray). (C) The *WUS-CLV* negative feedback regulatory pathway maintains the pluripotent stem cells in the CZ (pink) but also restrict the size of the SAM. *WUS* is also involved in regulating cytokinin at the SAM. It promotes cytokinin (CK) responses by repressing Type A ARR (?), a negative response factor of cytokinin. At the same time, cytokinin also induces *WUS* expression in the OC (blue). However, *WUS* represses the expression of LOG4, a cytokinin synthesis gene, in the CZ to inhibit cell division of these stem cells.
(A) and (C) were adapted from (Kitagawa and Jackson, 2019).

bear small, disorganized SAM , suggesting *WUS* promotes stem cell fate (Mayer *et al.*, 1998). WUS proteins can move from OC to the CZ to activate a gene named *CLAVATA3* (*CLV3*), which has opposite function as *WUS* by promoting differentiation of the cells at the shoot apex (Clark, Running and Meyerowitz, 1995; Fletcher *et al.*, 1999; Yadav *et al.*, 2011; Daum *et al.*, 2014). The *clv*3 mutants have enlarged SAM and produce club-shaped siliques. *CLV3* encodes a small peptide that travels back to the OC, where it can be perceived by several receptors: the *CLAVATA1* (*CLV1*) leucine-rich repeat receptor-like kinase (LRR-RLK); the *CLAVATA2* (*CLV2*) LRR-receptor like protein and CORYNE (CRN), a CLV2 co-receptor, to repress *WUSCHEL* expression (Figure1.1 C). This negative feedback regulation allows preservation of stem cell pool size but also limit cell division at the SAM (Clark, Williams and Meyerowitz, 1997; Jeong, Trotochaud and Clark, 1999; Schoof *et al.*, 2000; Müller, Bleckmann and Simon, 2008; Ogawa *et al.*, 2008). Besides the *WUS-CLV* pathway, there are many other factors influencing SAM size. For instance, the plant hormones cytokinin. Exogenous cytokinin was found to increase shoot meristem size in corn embryos (Giulini, Wang and Jackson, 2004). Plants with reduced cytokinin showed slow shoot growth and triple mutants of cytokinin receptors have smaller SAMs (Kieber, 2002; Higuchi *et al.*, 2004). Interestingly, cytokinin also forms a feedback loop with *WUS*: *WUS* expression can be activated by type-B cytokinin response regulators (RRs) while *WUS* promotes cytokinin responses at the shoot apex by repressing a type-A RR, *ARR7*, a negative regulator of cytokinin response (Figure 1.1C) (Leibfried *et al.*, 2005; Zhang, May and

Irish, 2017). Cytokinin induces *WUS* expression in the OC through a cytokinin receptor, *ARABIDOPSIS HISTIDINE KINASE4* (*AHK4*), which exhibits overlapping expression domains as *WUS* (Gordon *et al.*, 2009). Though it seems that cytokinin forms a positive feedback loop with *WUS*, it was reported that *WUS* represses cytokinin biosynthesis genes (the *LOG* genes) in the cells sitting at the topmost layer of SAM (Chickarmane *et al.*, 2012). The complex regulations of cytokinin and *WUS* are great examples of how plant SAM finetune gene expression to maintain and restrict the stem cell pool, allowing healthy growth to occur.

1.1.2 Root apical meristem (RAM): structure and regulation of development

While the SAM giving rise to all the above-ground tissues, growth is also happening at another apex buried under the ground, the root. *Arabidopsis* root can be divided into three zones: the meristematic zone (MZ), the elongation zone (EZ) and the differentiation zone (DZ) (Figure1.2 A). The new cells are produced in the MZ and enter the EZ to elongate and prepare themselves for differentiation at the DZ. Similar to the SAM, there are a group of cells near the tip of the root called the root apical meristem (RAM) or the MZ. However, the cells at the RAM are arranged differently from SAM. The quiescent center (QC) at the root tip contains a few slowly dividing stem cells (Figure1.2 A-C). These cells give birth to daughter cells that become initials (stem cells) for different parts or layers of the root. Together, the QC and the initials form the stem cell niche (Petricka, Winter and Benfey, 2012). These initials give rise to the cell files (circular layers) at the proximal part of the root:

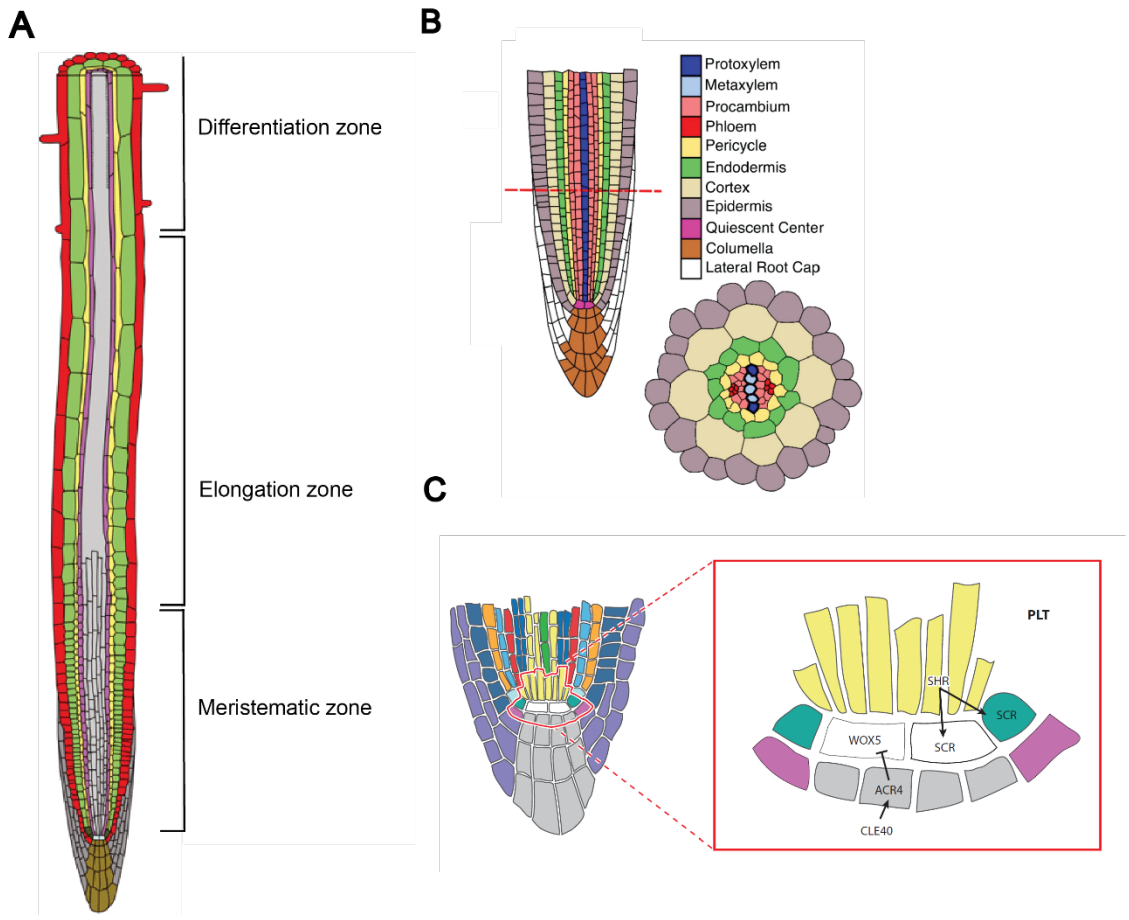

Figure 1.2: The organization and genetic regulation of *Arabidopsis* RAM.
(A) *Arabidopsis* root is divided into three major zones: meristematic zone, elongation zone and differentiation zone (labeled with brackets). (B) Diagrams showing cell organizations in the RAM. The cells are aligned along the length of the root. Different cell types are marked with different colors. (C) The maintenance of QC (white cells in magnified region) and initials (colored cells in magnified region) is regulated by the *WOX5-CLE40* pathway, transcription factors SHR, SCR and PLTs.
(A) was adapted from (Jin et al., 2013).
(B) was adapted from (Vaughan-Hirsch, Goodall and Bishopp, 2018).
(C) was adapted from (Petricka, Winter and Benfey, 2012).

epidermis, cortex, endodermis, pericycle and stele (vascular tissues), and the columella cells at the more distal part of the root (Figure1.2 B).

Though the structures are distinct from the SAM, the regulations of stem cell maintenance in RAM share some similarities. *WUSCHEL-RELATED HOMEOBOX5* (*WOX5*), a *WUS* homolog, is expressed in the QC and helps the QC to maintain

quiescence. *WOX5* suppresses cell division in QC by repressing the expression of a cyclin gene, *CYCD3;3* (Forzani *et al.*, 2014). *WOX5* also maintains stem cell identities of the surrounding initials in a non-cell-autonomous way. In the *wux5* mutant, the columella stem cells seem to lose their stem cell identity and acquire differentiated-cell like phenotypes (Sarkar *et al.*, 2007). The expression of *WOX5* is restricted to the QC in a similar manner to *WUS* in the shoot OC (Figure1.2 C). *CLAVATA3/ESR-RELATED 40* (*CLE40*), a gene encodes a peptide closely related to CLV3, represses *WOX5* expression through the receptor-like kinase ARABIDOPSIS CRINKLY4 (ACR4) and confers *WOX5* expression to the QC (Stahl *et al.*, 2009). Besides the *WOX5-CLE40* pathway, there are other factors that contribute to the maintenance of root stem cells. Loss of function at the *SHORT ROOT* (*SHR*) and *SCARECROW* (*SCR*) loci reduces the root length of *Arabidopsis* seedlings due to defects in QC (Benfey *et al.*, 1993; Laurenzio *et al.*, 1996; Wysocka-Diller *et al.*, 2000), indicating that these two GRAS family of transcription factors are necessary for the RAM functions. Interestingly, *SHR* is expressed in the stele and moves to the adjacent layer (QC, cortex/endodermis initials and daughter cells, endodermis) to induce *SCARE CROW* (*SCR*) expression (Helariutta *et al.*, 2000; Nakajima *et al.*, 2001; Levesque *et al.*, 2006). SHR then forms a complex with SCR to maintain the stem cell pools (Cui *et al.*, 2007).

In parallel with *SHR* and *SCR*, AP2-domain transcription factor PLETHORAs (PLTs) function in the meristematic zone to maintain QC identity and activate division in the initials in a dosage-dependent manner. In other words, *PLT*s form a maximum at the QC to promote stem cell identity and lower expression of *PLT*s in the initials allow

cell division to occur. Interestingly, ectopic expression of *PLT*s were able to induce root formation at the shoot, suggesting the critical role of PLTs in specifying root identity. The double mutant of *plt1;plt2* has much shorter root and reduced RAM size. *PLT*s also regulate the expression of auxin transporter PIN-FORMED (PINs). The *PIN* genes are downregulated in the *plt* mutants. So PLT promotes root stem cells by promoting auxin maximum at the root tip, which is consistent with auxin forming a similar gradient as *PLT*s (Aida *et al.*, 2004; Galinha *et al.*, 2007). Application of auxin promotes the root initiation but inhibits the root elongation (Thimann, 1936). It was believed that auxin was synthesized in the shoot and transported to the root through vascular tissues. However, auxin synthesis genes are also found expressed in the root stem cell, suggesting local auxin synthesis in the root (Gälweiler *et al.*, 1998; Blilou *et al.*, 2005; Ljung *et al.*, 2005; Stepanova *et al.*, 2005, 2008; Grieneisen *et al.*, 2007). In addition, auxin appears to regulate *PLT* expression, forming a positive feedback loop. Specifically, *PLT*s are thought to be activated by auxin through the auxin response factors MONOPTEROS (MP) and NONPHOTOTROPIC HYPOCOTYL4 (NPH4). help stabilizing the auxin maximum (Petricka, Winter and Benfey, 2012). Together, auxin and *PLT*s specify and maintain the stem cell niche at the root tip and allow cells to divide only upon their exiting the stem cell niche. Cytokinin is an important phytohormone in plant meristems. One interesting observation is the opposite roles cytokinin plays in root vs. shoot. Exogenous application of cytokinin reduces the meristem size in root but increases meristem size in shoot. In root, cytokinin and auxin work antagonistically. Cytokinin promotes cell

differentiation at the transition zone (TZ), which is located between the MZ and the EZ (Miyawaki, Matsumoto-Kitano and Kakimoto, 2004; Dello Ioio *et al.*, 2007). Cytokinin biosynthesis in the root is regulated by a family of transcription factors, the class III homeodomain-leucine zipper (HD-ZIP III). In Arabidopsis, the *HD-ZIP III* family has five members: *PHABULOSA* (*PHB*)*, PHAVOLUTA* (*PHV*)*, REVOLUTA* (*REV*)*, CORONA* (*CRN*)/*ATHB15* and *ATHB8*. They are involved in adaxial/abaxial polarity determination of lateral organs and vasculature patterning in plants. High expression of *HD-ZIP III*s induces metaxylem formation while downregulation of *HD-ZIP III*s promotes protoxylem formation. All members of *HD-ZIP III*s are targets of miR165/166. (McConnell and Barton, 1998; Emery *et al.*, 2003; Tang *et al.*, 2003; Zhong and Ye, 2004; Kim *et al.*, 2005; Zhou *et al.*, 2007).

The *PHB* gain-of-function mutant *phb-1d* showed short root and small RAM phenotypes. The expression of *PHB* is upregulated and broadened in the *phb-1d* mutant. Similar phenotypes have been found in the *PHV* gain-of-function *phv-1d*. These phenotypes are reminiscent of root treated with exogenous cytokinin (McConnell and Barton, 1998; Dello Ioio *et al.*, 2007; Dello Ioio *et al.*, 2012), suggesting that the phenotype of HD-ZIP III gain-of-function could be mediated by an increase of cytokinin. Indeed, it was demonstrated that PHB could activate the transcription of *ISOPENTENYLTRANSFERASE 7* (*IPT7*), a rate-limiting enzyme for cytokinin synthesis, suggesting that PHB directly regulates cytokinin synthesis in root. However, cytokinin produced in the vasculature restricts the expression of *PHB* and the negative regulator of *PHB*, *miR165* and such regulations may provide

robustness against cytokinin fluctuations in the root and help balance cell proliferation and differentiation (Dello Ioio *et al.*, 2012).

Although much is known about the *WUS-CLV* and *HD-ZIP III* transcription factors in regulating plant meristems, their relationship with cell cycle regulation is not well established. How did stem cells remain quiescent and how the existing regulators interact with cell cycle regulators are not well known. My work focused on this area using TSO1, a putative plant cell cycle regulatory complex component, as an entry point.

1.2 Arabidopsis *TSO1 and its role in meristem development*

1.2.1 *TSO1* encodes a transcription factor with cysteine-rich repeats

TSO1 was discovered from an EMS mutagenesis screen (Liu, Running and Meyerowitz, 1997; Hauser, Villanueva and Gasser, 1998). The strong allele *tso1-1* was isolated for its severe phenotypes at the shoot. The *tso1-1* plants have highly fasciated shoot apical meristems and lack most of the floral organs, thus they are sterile. *TSO1* was then cloned and subsequently proven to form a regulatory module

TCR motif: C-X-C-X(4)-C-X(3)-Y-C-X-C-X(6)-C-X(3)-C-X-C-X(2)-C
Hinge: R-N-P-X-A-F-X-P-K

Figure 1.3: Structure of *TSO1*
A simplified presentation of *TSO1* protein structure. The conserved sequence of TCR motif and Hinge motif are listed. The number marked the amino acid position.

with MYB3R1 to control cell cycle at the SAM and RAM (Hauser *et al.*, 2000; Song *et al.*, 2000; Wang *et al.*, 2018).

Arabidopsis TSO1 encodes a nuclear protein with two cysteine-rich repeat motifs (TSO1 Cysteine Rich motif or TCR motif) separated by a conserved hinge region (Figure 1.3) (Song *et al.*, 2000). Together, they are named as cysteine-rich repeats domain. The TCR motif has 9 conserved cysteine with invariable spacing (Figure1.3), which binds zinc and then DNA (Andersen *et al.*, 2007; Marceau *et al.*, 2016). Members of the cysteine-rich repeats domain protein family are found in both plants and animals. There are 8 members in *Arabidopsis thaliana*, which can be grouped into two groups based on domains outside the cysteine-rich repeats domain. *TSO1*, *SOL2* and *SOL1* fall into the first group (type I) while the rest 5 (*TCX4, TCX5, TCX6, TCX7* and *TCX8*) fall into the second group (type II).

1.2.2 *tso1* mutants exhibit defects in meristem development and *tso1* alleles can be categorized into two classes

All 9 alleles of *tso1* mutants are recessive mutations and they can be grouped into 2 classes. *tso1-1* and *tso1-2* are Class I mutations. Both are missense mutations that convert one conserved cysteine in the TCR motif to a tyrosine and both exhibit strong phenotypes (Sijacic, Wang and Liu, 2011). The *tso1-1* mutants exhibit developmental defects in both floral meristems and inflorescence meristems (Figure1.4 A and B), leading to sterility. The inflorescence meristems of *tso1-1* are frequently fasciated while the mutant floral meristems fail to give rise to normal floral organs except sepals and remain callus-like (undifferentiated). The fasciation observed at the SAM

is caused by the split of one meristem into two or multiple meristems rather than

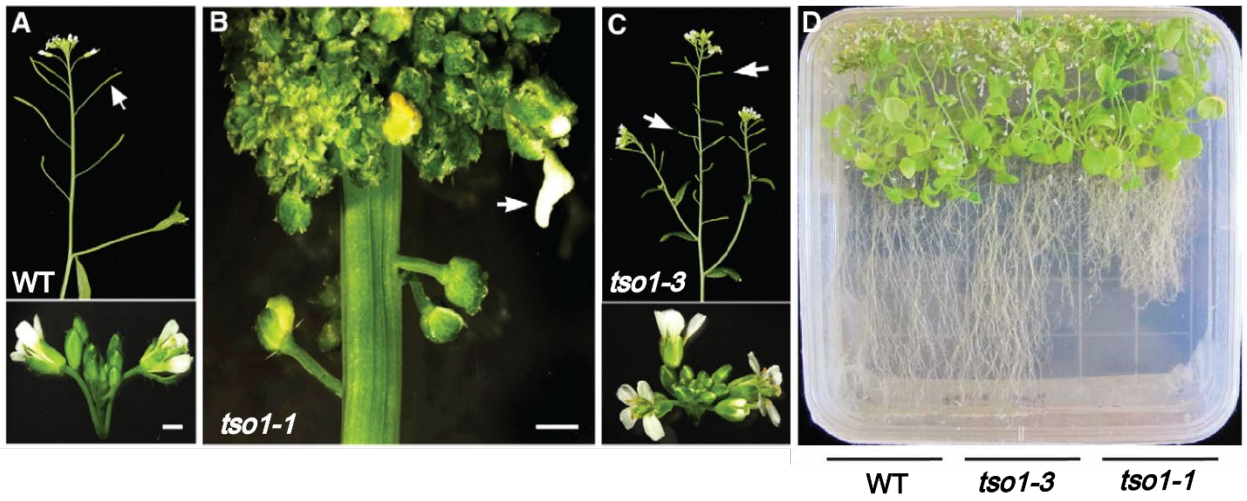

Figure 1.4: *tso1-1* (Class I) plants exhibit shoot apical meristem fasciation and short root phenotypes while Class II mutations of *TSO1* cause fertility defect.
(A) A wild type (*Landsberg erecta* or L*er*-0) plant showing normal shoot apical meristem and normal flowers. A fertile silique is indicated by the white arrow. (B) A *tso1-1* (type I) plant showing highly fasciated shoot meristem and failure of floral organ formation. (C) A *tso1-3* (type II) plant with normal SAM and flowers. Reduced fertility indicated by the short siliques (white arrow). (D) The roots of *tso1-1* plants are shorter than wild type plants. The *tso1-3* plants have no root phenotype Scale bar in A and B: 500 µm
All pictures were adapted from (Sijacic, Wang and Liu, 2011; Wang *et al.*, 2018).

enlargement of a single meristem. Electron microscopy of *tso1-1* floral meristem sections showed large and aberrant nuclei, elevated DNA content and abnormal cell plate formation, indicating defects in cell division (Liu et al 1997; Song et al 2000). *tso1-1* plants have short root phenotype resulting from the reduction in meristem size and possibly early differentiation of the stem cells (Figure1.4 D) (Wang *et al.*, 2018). Therefore, *TSO1* seems to cause opposite defects at the SAM and RAM.

The rest of the *TSO1* mutant alleles (*tso1-3* to *tso1-9*) fall into Class II. The Class II mutants, represented by *tso1-3* plants, exhibit weaker phenotypes than the Class I plants (Figure1.4 C). *tso1-3* is a nonsense mutation that generates truncated *TSO1* transcripts lacking the hinge motif and the second TCR motif (Song *et al.*, 2000).

tso1-3 plants have normal inflorescence meristems and can develop normal flowers. However, these plants have reduced fertility. Closer examination of the reproductive organs revealed that *tso1-3* plants produce ovules without the embryo sac (Hauser, Villanueva and Gasser, 1998). These results agree with the phenotypes observed in another Class II mutant, the *tso1-5* mutant. In addition to similar defects in ovules as *tso1-3* plants, the pollen grains in *tso1-5* are enlarged and collapsed (Andersen *et al.*, 2007). Together, we conclude that Class II *tso1* mutant plants are defective not only in the female gametes but also in the male gametes. Taken together, the analysis of two classes of *tso1* mutants indicates that *TSO1* is involved in regulating reproductive organ development in *Arabidopsis.*

It was puzzling why the missense *tso1-1* causes more severe phenotypes? The mystery has been resolved by knocking down *tso1-1* transcript using artificial microRNA. The resulting *tso1-1; amiRNA* plants produce normal flowers with reduced fertility, which resembles *tso1-3* (Class II) (Sijacic, Wang and Liu, 2011). In addition, 3 intragenic suppressors were isolated from a *tso1-1* suppressor screen. These alleles were named as *tso1-7, tso1-8* and *tso1-9* (Wang *et al.*, 2018). These findings suggest that *tso1-1* is a recessive antimorphic allele, which not only loses its own function but also interferes with the function of its paralogs such as *SOL2*. Specifically, double mutants of *sol2; tso1-3* showed strong phenotypes similar to those of *tso1-1*. Moreover, a BiFC experiment showed that SOL2 interacts with *TSO1-1* mutant protein but not the wild type TSO1. In summary, *tso1-1* is a recessive antimorphic allele which interferes with *SOL2* function by physical interaction, leading to a stronger phenotype than *tso1* null.

1.2.3 The animal homologs of TSO1 are cell cycle regulatory proteins

The animal homolog of *TSO1*, LIN54, is a component of the DREAM complex (Sadasivam and DeCaprio, 2013a; Fischer and Müller, 2017). LIN54 is homologous with *TSO1* only within the cysteine-rich repeats domain. The animal DREAM complex is a critical cell cycle regulator, acting both as a repressor and an activator of cell cycle genes depending on its interactors. The core complex of the DREAM complex, named as the MuvB complex or MuvB core (Korenjak *et al.*, 2004; Harrison *et al.*, 2006), consists of the core subunits of LIN54, the human homolog of TSO1, LIN53/RBBP4, LIN9, LIN37, and LIN52 (Litovchick *et al.*, 2007). In mammalian cells, the MuvB core can associate with the retinoblastoma (RB) family members (P107 and p130), the E2F transcription factors and their dimerization partners (DP1-3) to form the DREAM complex. This complex represses G_1/S genes, thus preventing cell cycle entry. In G_2/M phase, the MuvB binds to B-Myb transcription factor instead to form MMB complex to promote mitotic gene expression (Litovchick *et al.*, 2007; Sadasivam, Duan and DeCaprio, 2012). MuvB is an evolutionarily conserved complex. It has been identified in fly, worm, and *Arabidopsis* in addition to mammalian cells (Lewis *et al.*, 2004; Harrison *et al.*, 2006; Litovchick *et al.*, 2007; Schmit *et al.*, 2007; Kobayashi *et al.*, 2015). All of the homologs of the MuvB core have been found in plants and several DREAM-like complexes have been identified in *Arabidposis* (Ning *et al.*, 2020; Lang *et al.*, 2021). Additionally, plants have more copies of each of the complex components (Table1.1). For example, there are eight *Arabidopsis* homologs of LIN54 and five homologs of B-Myb. The existence of multiple paralogous genes coding each of the DREAM

component could potentially contribute to different isoforms of the DREAM/MMB complex, acting in different developmental contexts. So far, the plant DREAM-like complexes have been found to regulate meristem development, reproduction, stomata development, DNA methylation and response to DNA damage (Liu, Running and Meyerowitz, 1997; Hauser, Villanueva and Gasser, 1998; Song *et al.*, 2000; Sijacic, Wang and Liu, 2011; Wang *et al.*, 2018; Simmons *et al.*, 2019; Ning *et al.*, 2020; Lang *et al.*, 2021). These findings support the hypothesis that different forms of plant DREAM function in different biological processes.

Another distinct feature of plant DREAM-like complexes is that they seem to have components not found in the animal cells. Previously, two plant DREAM-like complexes were found to contain a cyclin-dependent kinase (CDK) CDKA;1, and one plant DREAM-like complex contains an uncharacterized protein encodes by AT2G40630 (*DRC2*) (Kobayashi *et al.*, 2015; Ning *et al.*, 2020). The presence of CDKA;1 in the purified complex suggests that the plant DREAM-like complex may regulate cell proliferation through somewhat different mechanisms from the animal DREAM complex. For instance, the plant MuvB core may associate with various CDKs to directly control cell proliferation in a developmental stage-specific or tissue-specific manner.

Like plants, disruptions of the DREAM/MMB complex in animal cells usually lead to severe developmental defects or cancer. Mutating either homolog of LIN37 (Mip40), LIN54 (Mip120

) or LIN9 (Mip130) leads to sterility in flies (Beall *et al.*, 2007). The loss of both retinoblastoma protein (pRb) and Rb-like (p107/p130) induces retinoblastoma in mice while overexpression of B-Myb was found in many cancers including breast cancer and colorectal cancer, and often associated with poor patient outcomes (Musa *et al.*, 2017; Wu *et al.*, 2017). Understanding the function of the DREAM/MMB complex during tumorigenesis has become an interesting research field. A recent finding revealed novel mechanisms of how overexpression of B-Myb disrupts cell cycle

Human	AGI	Alias
B-Myb	AT4G32730	MYB3R1
	AT5G00540	MYB3R2
	AT3G09370	MYB3R3
	AT5G11510	MYB3R4
	AT5G02320	MYB3R5
E2F	AT2G36010	E2FA
	AT5G22220	E2FB
	AT1G47870	E2FC
	AT5G14960	E2FD/DEL2
	AT3G48160	E2FE/DEL1
	AT3G01330	E2FF/DEL3
DP	AT5G02470	DPA
	AT5G03415	DPB
RB	AT3G12280	RBR1
LIN9	AT5G27610	ALY1
	AT3G05380	ALY2
	AT3G21430	ALY3
LIN54	AT3G22780	TSO1
	AT4G14770	TCX2/SOL2
	AT3G22760	TCX3/SOL1
	AT3G04850	TCX4
	AT4G29000	TCX5
	AT2G20110	TCX6
	AT5G25790	TCX7
	AT3G16160	TCX8
LIN37	AT1G04930	LIN37A
	AT2G32840	LIN37B
LIN52	AT2G45250	LIN52A/DRC1
	AT4G38280	LIN52B
RBBP4	AT5G58230	MSI1
	AT2G16780	MSI2
	AT4G35050	MSI3
	AT2G19520	MSI4
	AT4G29730	MSI5

Table 1.1: *Arabidopsis* homologs of the DREAM complex components
This table presents the plant homologs of each DREAM components. The mammalian DREAM protein names are listed in the first column. AGI stands for *Arabidopsis* gene ID and Alias stands for the annotated name of the corresponding gene. The Muv B core genes are shaded in light green color.
The table was adapted from (Lang *et al.*, 2021).

(Iness *et al.*, 2019). The over-accumulated B-Myb can interfere with DREAM assembly by affecting phosphorylation of LIN52, an essential process for forming the DREAM complex, which may lead to the poor patient outcomes.

LIN54, the TSO1 homolog, is the only component in the MuvB core that interacts with DNA. It specifically recognizes and binds to the consensus sequence TTYRAA in the CHR (cell cycle genes homology region) in the target promoters (Marceau *et al.*, 2016). This binding enables DREAM/MMB complex to be recruited to a large numbers of cell cycle genes, for example, the G_2/M cell cycle genes cdc2 in human cells (Schmit *et al.*, 2007; Müller *et al.*, 2014, 2016). The phenotypes observed in *tso1-1* plants are consistent with the phenotypes found in animal systems. For instance, flies with the *TSO1* homolog (Mip120) knock-out are sterile; LIN54 depletion cells went through prolonged G_2 phases (Beall *et al.*, 2007; Schmit, Cremer and Gaubatz, 2009). It seems that *TSO1* may function in a similar manner as LIN54 in plant. The discoveries of several potential plant DREAM complex support this hypothesis (Kobayashi *et al.*, 2015; Wang *et al.*, 2018; Ning *et al.*, 2020; Lang *et al.*, 2021). Nevertheless, little is known about the precise functions of these MuvB core proteins in plants.

1.2.4 A mutagenesis screen identified *myb3r1* a suppressor of *tso1-1*

To understand how *TSO1,* a member of the plant DREAM complex ,regulates cell division in the context of shoot meristem development, a former graduate student set out to identify genetic suppressors of *tso1-1* through mutagenesis screens (Wang *et al.*, 2018). Mutations in genes downstream of TSO1 could potentially suppress *tso1-1* phenotype. Since *tso1-1* is sterile, an inducible copy of wild type *TSO1* was

introduced in to plants homozygous for *tso1-1* in order to obtain homozygous mutant seeds. The full length *TSO1* cDNA driven by the 35S promoter was fused to a rat glucocorticoid receptor (GR) and transformed into *tso1-1* heterozygous plants. The TSO1-GR fusion proteins are retained in the cytoplasm without dexamethasone (DEX) treatment. When supplied with DEX, the fusion proteins can enter the nucleus and rescue *tso1-1* phenotype, generating thousands of *tso1-1* homozygous mutant seeds. These seeds were then treated with Ethyl methanesulfonate (EMS) and screened for the restoration of normal meristem and fertility without DEX application.

Isolated from the screen were 45 suppressors. 32 of the suppressors were mapped to *MYB3R1*, one of the R1R2R3-MYB (MYB3R) genes that shares homology with animal B-Myb transcription factors (Wang *et al.*, 2018). *MYB3R1* and its close *Arabidopsis* homolog *MYB3R4* are activators for G_2/M phase genes. For instance, *MYB3R1* and *MYB3R4* activate *KNOLLE* to promote cytokinesis (Haga *et al.*, 2007, 2011). Knock-out of *MYB3R1* in *tso1-1* can suppress both shoot and root phenotype and restore fertility (Figure1.5 A, B and C). It has been found that *MYB3R1* is ectopically expressed and overexpressed at both SAM and RAM in *tso1-1* plants (Figure1.5 D), indicating that *TSO1* represses *MYB3R1* transcription in the wild type plants. Thus, any mutations removing the excessive *MYB3R1* can suppress *tso1-1* phenotypes.

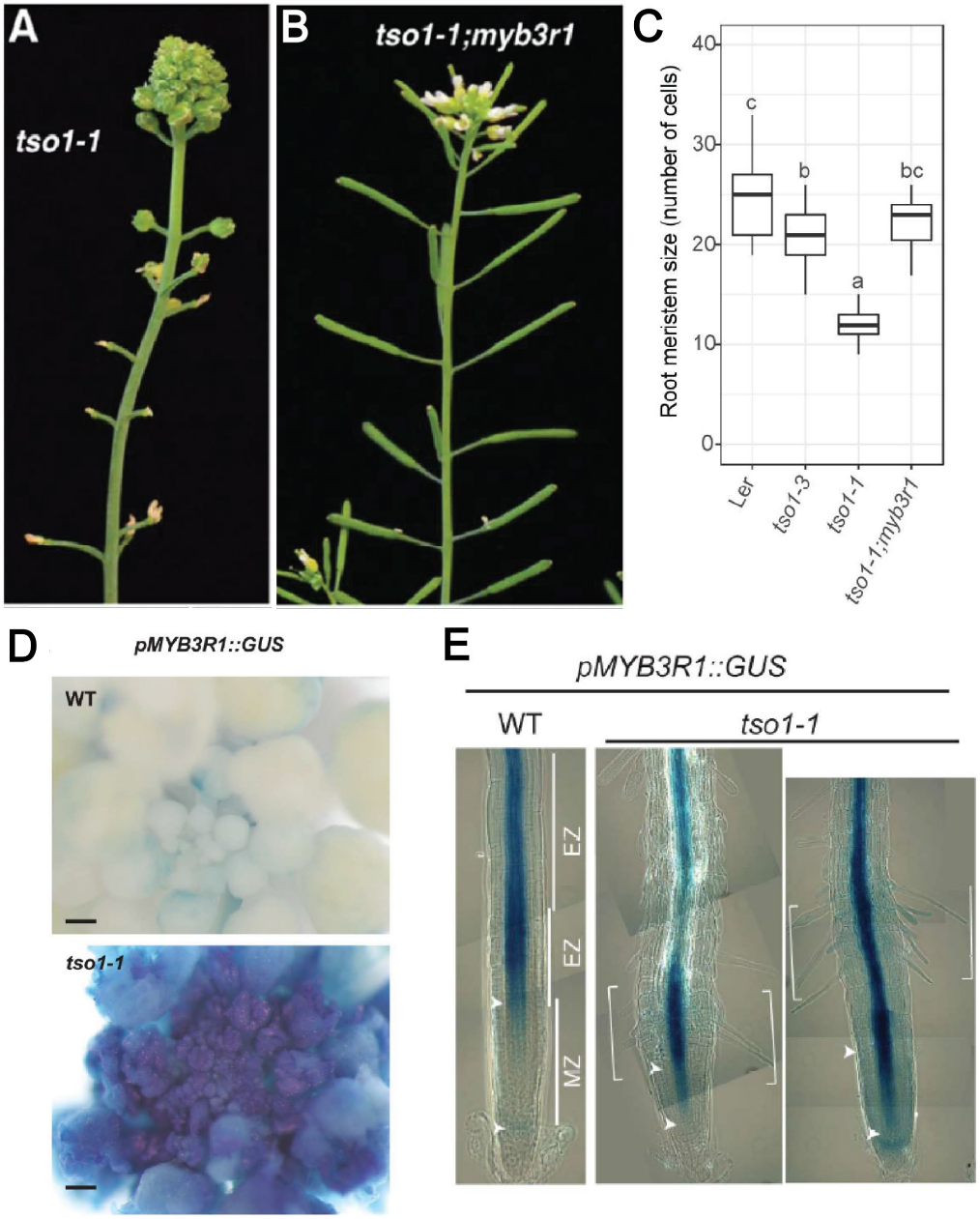

Figure 1.5: Overexpression of *MYB3R1* mediates *tso1-1* phenotypes.
(A) An inflorescence of a homozygous *tso1-1* mutant plant. (B) An inflorescence of *tso1-1; myb3r1* double mutant. The mutation in *MYB3R1* suppressed the fasciation and sterility of *tso1-1*. (C) Quantification of the RAM size. Mutating *MYB3R1* also suppressed the short root phenotype of *tso1-1*. (D) Staining of *pMYB3R1-GUS* in wild type (WT) and *tso1-1* SAM. Intense blue staining in *tso1-1* suggests overexpression of *MYB3R1*. (E) Staining of *pMYB3R1-GUS* in WT and *tso1-1* RAM (7dpg). Upper arrow: transition zone; lower arrow: QC; brackets: intense blue stain accompanied with emerging root hairs. Scale bar: 200 μm.
All pictures were adapted from (Wang *et al.*, 2018).

To further investigate the suppression mechanism, *35S::MYB3R1* has been transformed into wild type plants and *tso1-3* plants. Surprisingly, neither of the resulting plants resemble *tso1-1* phenotype. It seems that *tso1-1* phenotype is not solely mediated by misexpression of *MYB3R1*. Later, it was found that phosphomimic of MYB3R1 at S656 position enhanced *tso1-3* fertility defects but failed to phenocopy the SAM fasciation of *tso1-1* mutants (Wang *et al.*, 2018). It seems that overexpression of MYB3R1 is necessary but not sufficient to cause the *tso1-1* phenotype. A coimmunoprecipitation (Co-IP) experiment showed that TSO1 could physically interact with MYB3R1 to form a regulatory module, which agrees with previous publications on the MYB3R1 a component of the plant DREAM-like complexes.

The result of simply overexpressing MYB3R1 did not phenocopy the SAM fasciation of *tso1-1* led to the hypothesis that there might be other components in the TSO1-MYB3R1 regulatory module. Although several DREAM-like complexes were discovered in *Arabidopsis* seedlings and leaves, none has been reported in SAM or RAM where TSO1 and MYB3R1 are expressed. It suggests that plants may have multiple DREAM-like complexes present in different tissues to coordinate cell cycle with development. My work has been focused on exploring other components involved in the TSO1-MYB3R1 regulatory module. A144 was isolated from the previous suppressor screen and was later characterized as a unique *tso1-1* suppressor, indicating its role in the TSO1 regulatory pathway. The work will further our understanding of how plant meristems balance cell proliferation and differentiation

through manipulating regulatory networks of transcription factors and cell cycle machineries to develop and maintain their stem cell identities at the same time.

1.3 Cyclin genes and their roles in meristem development

1.3.1 The classification of plant cyclin genes

Cyclins, as the name indicates, has unique cycling expression patterns. The abundance of a cyclin protein oscillates throughout the cell cycle. Cyclins are important cell cycle regulators. They bind to CDKs to form cyclin-CDK complexes. This binding is critical for CDK activation and substrate recognition. Cyclin also helps to bring CDK into the nucleus as CDK usually lacks a nuclear localization signal (David-Pfeuty and Nouvian-Dooghe, 1996; Schafer, 1998). Cyclins can be divided into following categories according to their expression patterns, which also are indicators for their functions. G_1/S cyclins promote entry into the cell cycle, whereas S cyclins promote DNA synthesis, and M cyclins help cells to enter M phase. Cyclins with D-box domains are targeted for degradation after fulfilling their functions, making cell cycle irreversible.

Cyclins can be further classified according to their sequences, though they share poor homology in general. Based on the literature, there are 19 cyclins identified in human. Each can form a different complex with CDKs (Truman *et al.*, 2012). This number greatly expands in plants, such as *Arabidopsis,* that has 50 putative cyclin genes. These cyclins can be grouped into eight classes: *CYCA1-3*, *CYCB1-3*, *CYCC*, *CYCD1-7*, *CYCH*, *CYCL*, *CYCP1-4* and *CYCT* and 3 additional cyclins not belonging to these groups: *CYCJ18*, *SOLODANCERS* and *CYL1* (Figure1.6) (Menges *et al.*,

2005). The large number of cyclin genes brought great challenges when it comes to the analysis of their specific functions. In other words, single mutant is unlikely to show any phenotypes, making it hard to interpret the regulatory pathways each cyclin is involved in.

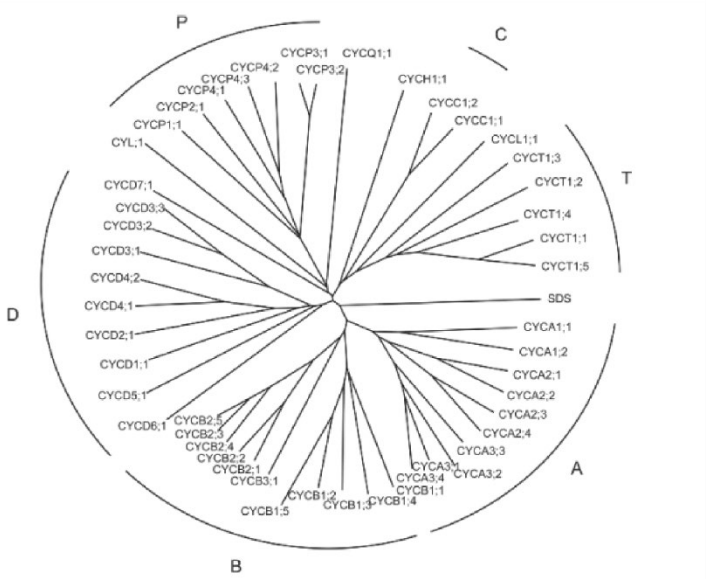

Figure 1.6: The phylogenetic tree of *Arabidopsis* cyclin genes.
Full length sequences of 50 *Arabidopsis* cyclins were used in the alignment. The unrooted neighbor-joining tree was based on multiple sequence alignment. Picture was adapted from (Nieuwland, Menges and Murray, 2007).

1.3.2 Functions of *Arabidopsis CYCA3*s

Plants are sessile organisms. They are not able to move from places to places to avoid environmental stresses. Therefore, plants need more flexible regulatory modules for its growth and reproduction. This may explain why the number of cyclins expanded in plants. Cyclins have been found to play important roles in plant development and stress responses.

Cyclins in the same class usually share some similarities in their functions. Though it is still hard to know the molecular function of each member, previous studies have

revealed some common functions of different classes plant cyclins. For instance, the expression of B-type cyclins (*CYCB*s) peak in early M phase (Menges *et al.*, 2005). They are most likely to regulate M phase. The expression of D-type cyclins is dependent on the presence of mitogens. Adding cytokinin or sucrose induces expression of *CYCD3;1* in plant cell cultures (Soni *et al.*, 1995). Does this indicate that D type cyclins mainly regulate G1/S cell cycle check point? In Arabidopsis, one of the *CYCB* genes was shown to function in male meiosis. Ectopic cell wall formation was found in the *cycb3;1* mutants, indicating that it prevents cell wall formation in *Arabidopsis* pollen mother cells (Bulankova *et al.*, 2013).

CYCA3 genes can be further divided into three subclasses: *CYCA1* (*CYCA1;1* and *CYCA1;2*), *CYCA2* (*CYCA2;1, CYCA2;2, CYCA2;3* and *CYCA2;4*) and *CYCA3* (*CYCA3;1*, *CYCA3;2*, *CYCA3;3* and *CYCA3;4*). *CYCA1* and *CYCA2* genes are mainly expressed in G_2/M while *CYCA3*s have diverse expression patterns (Menges *et al.*, 2005). For instance, the expression of *CYCA3;1* and *CYCA3;2* peaks in S phase, but *CYCA3;3* is exclusively expressed in the meiotic cells. These expression patterns suggest that *CYCA3;1* and *CYCA3;2* may play roles in the S phase while *CYCA3;3* might specifically function in the meiosis. Since *CYCA3;3* lacks a D-box domain, its degradation is not mediated by the anaphase-promoting complex (APC/C) but alternative mechanisms. Finally, *CYCA3;4* show different expression patterns in the Arabidopsis MM2d cell line and roots. *CYCA3;4* was found to have a constant expression in the MM2d cells. However, CYCA3;4 proteins mainly accumulate in the G_2/M phase in the root.

None of the single mutant of *CYCA3* genes showed significant phenotypes (Takahashi *et al.*, 2010; Bulankova *et al.*, 2013; Willems *et al.*, 2020). The *cyca3;1-1; cyca3;2-1* double mutant was indistinguishable from the wild type plant. Thus, overexpression has been used to reveal the potential functions of *CYCA3* genes. Overexpression of *CYCA3;1* and *CYCA3;2* caused early termination of the apical buds and the lateral branches grow better than the main shoots perhaps as a result of loss of apical dominance (Takahashi *et al.*, 2010). Overexpression of *CYCA3;4* caused short roots, defects in leaf growth, and fewer stomata (Willems *et al.*, 2020). One intriguing finding about these plant *CYCA3s* is that they seem to control the phosphorylation of RBR1, which is the homolog of animal Retinoblastdoma (RB) and a member of the DREAM complex . The plant CYCA3;1-CDKA;1 complex was shown to phosphorylate RBR1 *in vitro* and overexpression of *CYCA3;4* resulted in hyperphosphorylation of RBR1 in vivo (Takahashi *et al.*, 2010; Willems *et al.*, 2020). In a recent publication, mutations in *CYCA3;4* were shown to partially suppress *ccs52a2-1*'s phenotype in short root and reduced rosette leaf size (Willems *et al.*, 2020). The *CCS52A2* encodes a activator of the anaphase-promoting complex (Liu *et al.*, 2012). CYCA3;4 can be targeted to degradation by $APC/C^{CCS52A2}$ and hence proper degradation of CYCA3;4 by $APC/C^{CCS52A2}$ is necessary for normal meristem development. Meanwhile, mutating *CYCA3;1* and *CYCA3;2* was not able to suppress *ccs52a2-1*, indicating they may not be regulated by $APC/C^{CCS52A2}$ in this pathway. Meanwhile, efforts have been made to identify specific paring of *Arabidopsis* cyclins with their CDKs through yeast two hybrid assays and BiFC (Boruc *et al.*, 2010; Van Leene *et al.*, 2010). BiFC data showed that CYCA3;4 could interact with CDKA;1

and CDKB2;1, suggesting that CYCA3;4 may form functioning complexes with these two CDKs (Figure1.7).

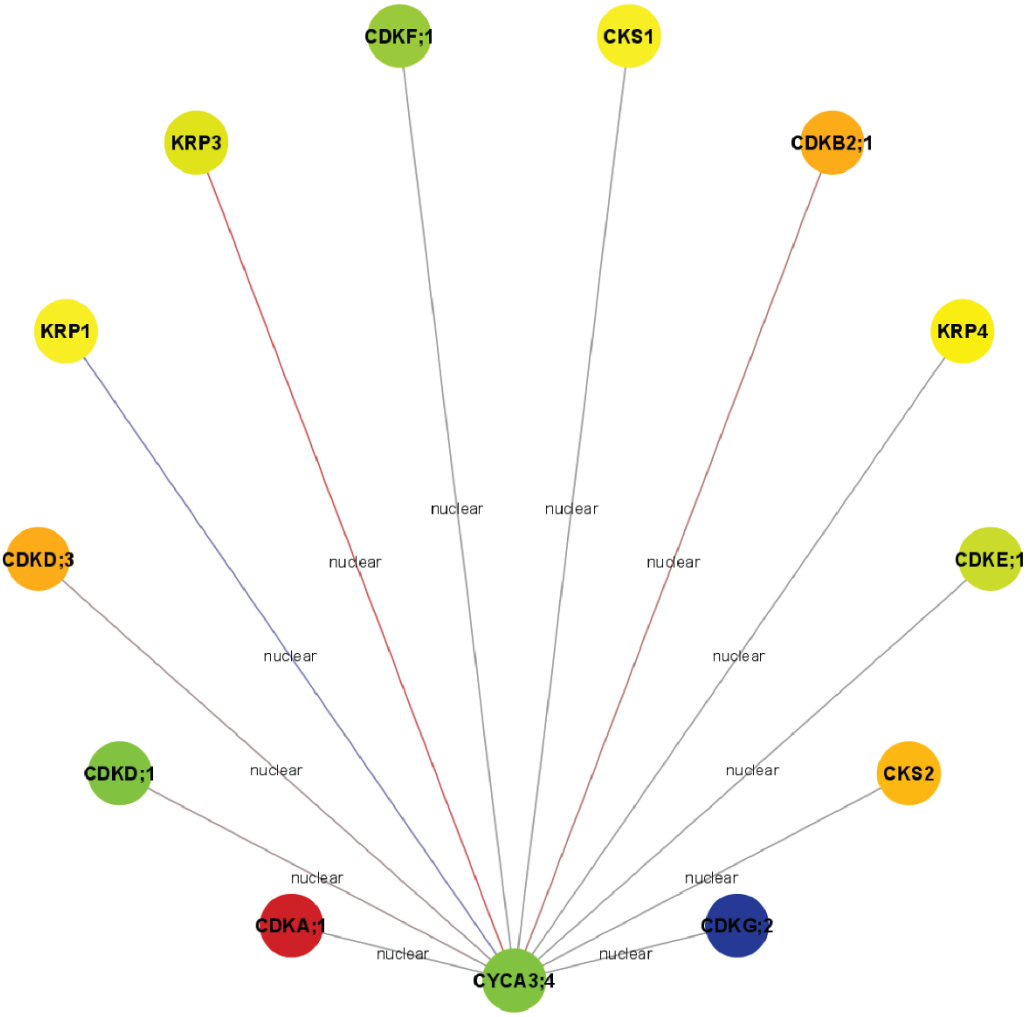

Figure 1.7: The protein-protein interaction network of CYCA3;4.
The protein-protein interaction network of CYCA3;4 was based on BiFC data. Each node represents a gene, and the lines represent interaction and correlation of expression (transcription level). Red: highly positively correlated; Blue: highly negatively correlated; Gray: interaction detected without any significant correlation. All interactions were detected in the nuclear, which are labeled with 'nuclear' on the lines.
Picture was adapted from (Boruc *et al.*, 2010)

My dissertation investigated a novel suppressor of *tso1-1* and identified a G-to-A mutation in a cyclin A gene, *CYCA3;4*, as the causal mutation. Using transgenic technique and transient expression assay, I showed that *CYCA3;4* was overexpressed in the *tso1-1* SAM and *TSO1* likely regulate the expression of *CYCA3;4* through regulating another *TSO1* target gene *MYB3R1*.

I discovered potential *TSO1* target genes through comparing the single cell RNA sequencing data of *tso1-1* root and wild type root. I found that the expression of the *HD-ZIP III* transcription factors and several cytokinin biosynthesis genes are increased in the *tso1-1* root. The *HD-ZIP III* genes are mainly overexpressed in the vascular cells of *tso1-1* while the ectopic expression of cytokinin biosynthesis genes is seen in vascular cells, endodermis and QC. The scRNA-seq data of *tso1-1* also provide rich resources to explore *TSO1* functions in regulating other plant hormones and transcription factors, which is not included in this dissertation.

Overall, my work demonstrates the molecular mechanisms of *TSO1* regulating shoot and root development through regulating a specific cyclin gene and cytokinin biosynthesis. It established *TSO1* as a critical regulator of plant meristem maintenance and development. The regulatory pathway revealed by my work furthered our understanding of how conserved cell cycle machineries are involved in plant development.

Chapter 2: Mutations in a A-type cyclin gene suppresses *tso1-1* shoot phenotype

2.1 Introduction

Plant meristems are responsible for generating all above and below ground tissues. Identifying gene regulatory circuitries that confer and maintain the "stem cell" property in plant meristems is fundamentally important. In plant shoot apical meristem (SAM), the *WUSCHEL (WUS)-CLAVATA (CLV)* negative feedback loop maintains the stem cell pool and limits the meristem size. Besides the *WUS-CLV3* pathway, there has been limited studies of other regulatory circuitries for SAM regulation, and little is known about how the stem cell pool regulation is integrated with the cell cycle regulation at SAM.

The DREAM/MMB complex is a master cell cycle regulator in both animals and plants (Sadasivam and DeCaprio, 2013b; Kobayashi *et al.*, 2015). The animal DREAM complex consists of Retinoblastoma (RB)-like proteins (P107 and p130), E2Fs and their dimerization partners DP1-3 and the MuvB core (LIN9, LIN37, LIN52, LIN54 and RBBP4). In animal quiescent cells, the DREAM complex prevents cells from entering cell cycles while in dividing cells, the MuvB core associates with B-Myb (also called MYBL2) instead of Rb-like to form the MMB complex that promotes the G2/M phase (Fischer and Müller, 2017). Recent studies revealed that the DREAM/MMB complex exists in plants as well. The *Arabidopsis* genome possesses essentially all the homologous genes of the DREAM/MMB complex components and the corresponding plant homologs can form similar complexes (Ning *et al.*, 2020; Lang *et al.*, 2021). Additionally, plants have more copies of each the

complex component. For example, there are eight Arabidopsis homologs of LIN54, named as *TSO1*, *SOL1*, *SOL2*, *TCX4, 5, 6, 7* and *8*, all of which encode two cysteine-rich CXC motifs separated by a linker region (Hauser *et al.*, 2000; Song *et al.*, 2000; Andersen *et al.*, 2007). The existence of multiple paralogous genes coding each of the DREAM component could potentially contribute to different isoforms of the DREAM/MMB complex, acting in different developmental contexts. Though biochemical characterizations have been performed on the possible combinations of the plant DREAM/MMB complexes, the functions of each complex and of each member of the complex remain largely unknown.

In animals, disruptions of the DREAM/MMB complex usually lead to cancer. The loss of both retinoblastoma protein (pRb) and Rb-like (p107/p130) induces retinoblastoma in mice (Wu *et al.*, 2017), while overexpression of B-Myb was found in many cancers including breast cancer and colorectal cancer, and often associated with poor patient outcomes (Musa *et al.*, 2017). While plants do not suffer from cancer, plant mutants defective in the DREAM/MMB components exhibit shoot meristem fasciation, an over-proliferation of SAM. In *Arabidopsis*, the *tso1-1*, an antimorphic mutation in the *Arabidopsis* homolog of LIN54, shows fasciated shoot apical meristems, and *tso1-1* mutant flowers fail to differentiate into floral organs and are sterile (Liu, Running and Meyerowitz, 1997; Sijacic, Wang and Liu, 2011; Wang *et al.*, 2018). Meanwhile, the cells in the *tso1-1* root apical meristem (RAM) exit cell cycle early, resulting in a short root phenotype, suggesting opposite effects of *TSO1* on shoot and root meristems. *tso1-3*, a loss-of-function allele, on the other hand, has weak phenotypes; it develops normal flowers and normal length root but exhibits

reduced fertility (Hauser *et al.*, 2000; Sijacic, Wang and Liu, 2011; Wang *et al.*, 2018). These two different mutant alleles of *TSO1* in *Arabidopsis* provide a useful tool to dissect DREAM/MMB function in the context of plant meristem regulation. To identify genes that may act in the same pathway as *TSO1,* we previously conducted a genetic screen for suppressors of *tso1-1* (Wang *et al.*, 2018). Seeds of *tso1-1* containing an inducible *TSO1* (*35S::TSO1-GR*) were mutagenized. When applied with dexamethasone (DEX), *tso1-1; 35S::TSO1-GR* M1 plants were able to overcome sterility and gave rise to M2 progeny, which were screened for suppressors. Thirty-two suppressors from the screen were found to reside in *MYB3R1*, which encodes one of the five *Arabidopsis* homologs of B-Myb. The work established that the wild type *TSO1* activity is required to repress *MYB3R1* expression to prevent SAM over-proliferation.

In this study, we characterized a second suppressor locus of *tso1-1* from the same genetic screen. We showed that mutations in an A-type cyclin named *CYCA3;4* suppressed *tso1-1* shoot fasciation and sterility to certain degrees. Further, *TSO1* and *MYB3R1* were shown to regulate the expression of *CYCA3;4*, and *CYCA3;4* overexpression enhances *tso1-3* phenotype. The work reveals the function of a specific cyclin in shoot meristem regulation and provides mechanistic insights into the function of the *TSO1-MYB3R1* regulatory module in shoot meristem regulation.

2.2 Results

2.2.1 A splice-site mutation in *CYCA3;4* suppresses *tso1-1* shoot phenotype

In order to identify new components of the *TSO1* regulatory pathway, a second suppressor locus, defined by a single allele *A144*, was analyzed. *A144* suppresses the shoot fasciation of *tso1-1* mutant and the fertility defects of both strong (*tso1-1*) and weak (*tso1-3*) alleles of *tso1* (Figure2.1). However, the suppression is not complete as *A144* only partially restores the fertility of *tso1-1*.

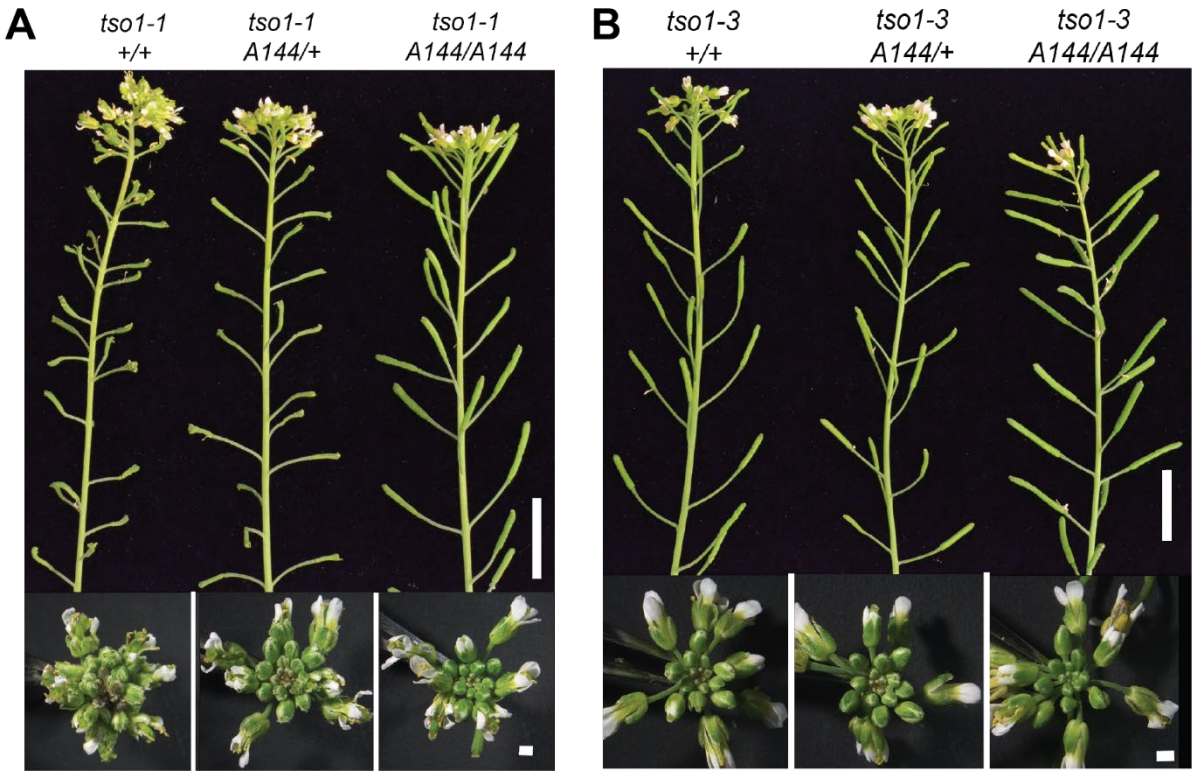

Figure 2.1 Homozygous *A144* mutation suppresses defects of *tso1-1* and *tso1-3*.
(A) Comparison of inflorescences and siliques among *tso1-1* plants heterozygous or homozygous for the *A144* mutation. The top panel illustrates suppression of fertility defects by homozygous *A144*. Arrowheads point at sterile carpels, and arrows indicate fertile siliques. Bottom images show shoot meristem fasciation in *tso1-1* and *tso1-1; A144/+* with more floral buds and wild type-like inflorescence in *tso1-1; A144/A144.* All plants in (A) contain the *35S::TSO1-GR* transgene but are not treated with DEX. (B) Comparison of inflorescences and siliques of a weak *tso1* allele, *tso1-3,* which has reduced fertility (top panel) but normal SAM (bottom). Homozygous *A144* further improves *tso1-3* fertility with longer and fuller siliques. Scale bars in A, B: 1cm in the upper panel and 1mm in the lower panel.

To isolate the gene defined by the *A144* suppressor, an F2 mapping population was created. Using the SIMPLE mapping pipeline (Wachsman *et al.*, 2017), *A144* was mapped to an A-type cyclin gene *CYCA3;4* on chromosome 1 (Figure2.2). A G-to-A mutation occurs in the last nucleotide of the first exon of *CYCA3;4*, however it is a synonymous mutation (E-to-E) (Figure2.3 A).

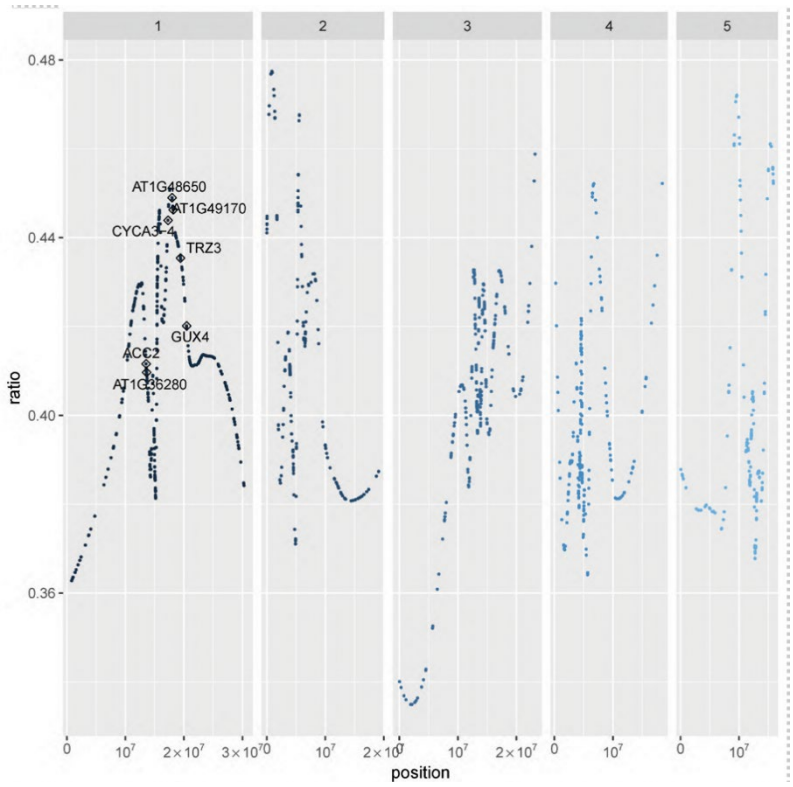

Figure 2.2 Mapping-by-sequencing result showing *CYCA3;4* the best candidate for *A144*.
An output plot from the SIMPLE pipeline (Wachsman et al., 2017) showing the allele frequency comparison between the unsuppressed and suppressed plants. *CYCA3;4* (AT1G47230) is located at the peak on Chromosome 1.

RT-PCR was used to examine if this mutation affects the splicing of *CYCA3;4* transcripts. A *CYCA3;4* transcript of wild-type size was not detected in the *A144* plants, but two transcripts of aberrant sizes were detected (Figure2.3 B). Sequence analysis of the RT-PCR products shows that the longer aberrant transcript retains the first intron while the shorter aberrant transcript used a cryptic splice donor site in the first exon. As both the aberrant transcripts contained premature stop codons, *A144* likely causes a non-functional *CYCA3;4*.

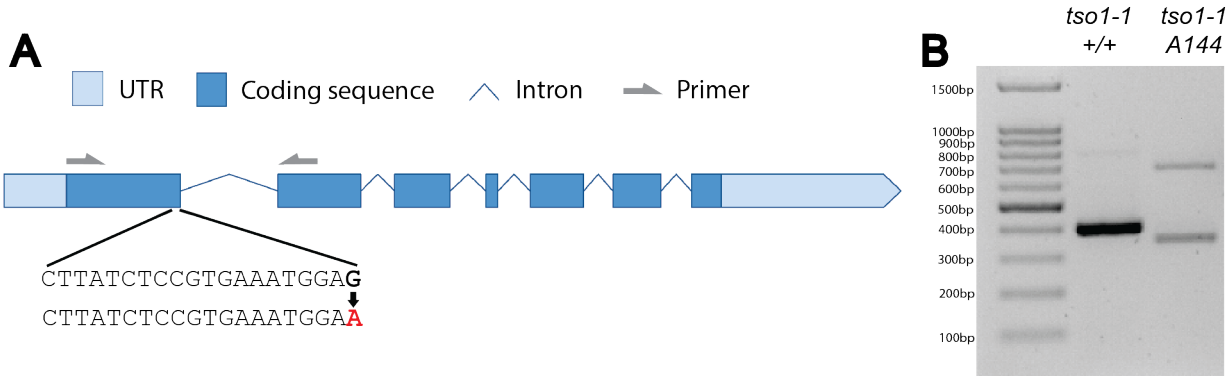

Figure 2.3 The G-to-A mutation affect splicing of *CYCA3;4* transcripts.
(C) Gene model of *CYCA3;4*. The G-to-A mutation is highlighted in red. (D) RT-PCR showing two aberrant transcripts in *tso1-1; A144*.

2.2.2 CRISPR/Cas9 mediated knockouts of *CYCA3;4* also suppress *tso1-1*

To confirm that the mutated *CYCA3;4* is indeed the causal mutation for *A144*, we conducted both complementation tests and CRISPR/Cas9 knockout of *CYCA3;4*. The genomic sequence of *CYCA3;4* (*gCYCA3;4;* from ~1.4 kb upstream to the end of 3'UTR) was transformed into the *A144* plants containing the *tso1-1* mutation. If the transgene rescues *A144*, the resulting transgenic plants should regain the *tso1-1* mutant phenotype, which was indeed observed including meristem fasciation and complete sterility (Figure2.4).

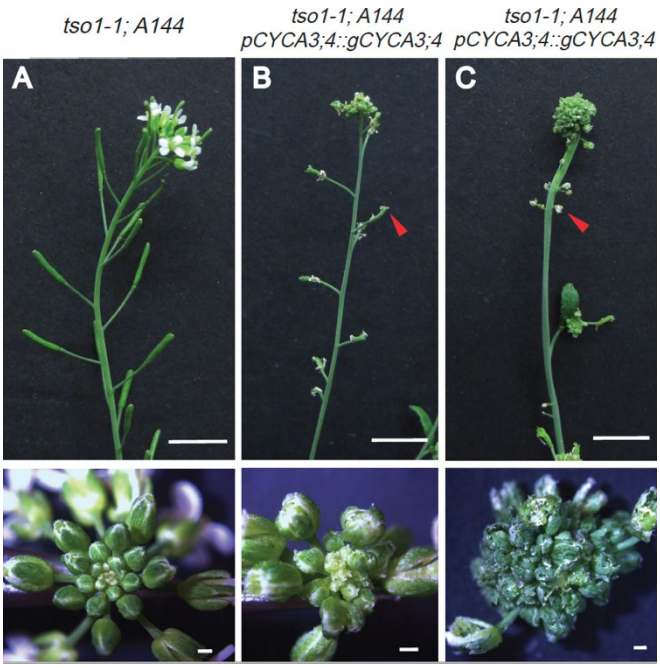

Figure 2.4 Complementation test confirming *CYCA3;4* as *A144*.
(A) Top panel shows a *tso1-1; A144* shoot with a normal inflorescence and fertile siliques. Bottom panel shows a top view of a wild type-like SAM in *tso1-1; A144*. (B)-(C) are two independent transgenic lines showing a loss of suppression due to their harboring the g*CYCA3;4* transgene. Note the sterile carpels (red arrowheads). The bottom panel shows top view of SAMs and reveals a severely fasciated SAM in C. Scale bars: 1cm in the top panes and 500µm in the lower panel.

Second, a CRISPR/Cas9 construct with a gRNA targeting the first exon of *CYCA3;4* was transformed into *tso1-1; 35S::TSO1-GR* plants. Several T_1 plants showed suppressed phenotypes even in the absence of DEX application (Figure2.5 A). These plants did not exhibit shoot fasciation and developed somewhat elongated siliques containing a few seeds, which contrasts with complete sterility of *tso1-1; 35S::TSO1-GR* plants in the absence of DEX (Figure2.5 B). Sequencing of the *CYCA3;4* locus in these plants showed either homozygous or biallelic mutations in *CYCA3;4* (Figure2.5 E). Together, these data strongly support that *CYCA3;4* defines the second suppressor

locus of *tso1-1,* and *A144* is renamed as *cyca3;4-4* (*cyca3;4-1, cyca3;4-2,* and *cyca3;4-3* were previously reported (Willems *et al.*, 2020)).

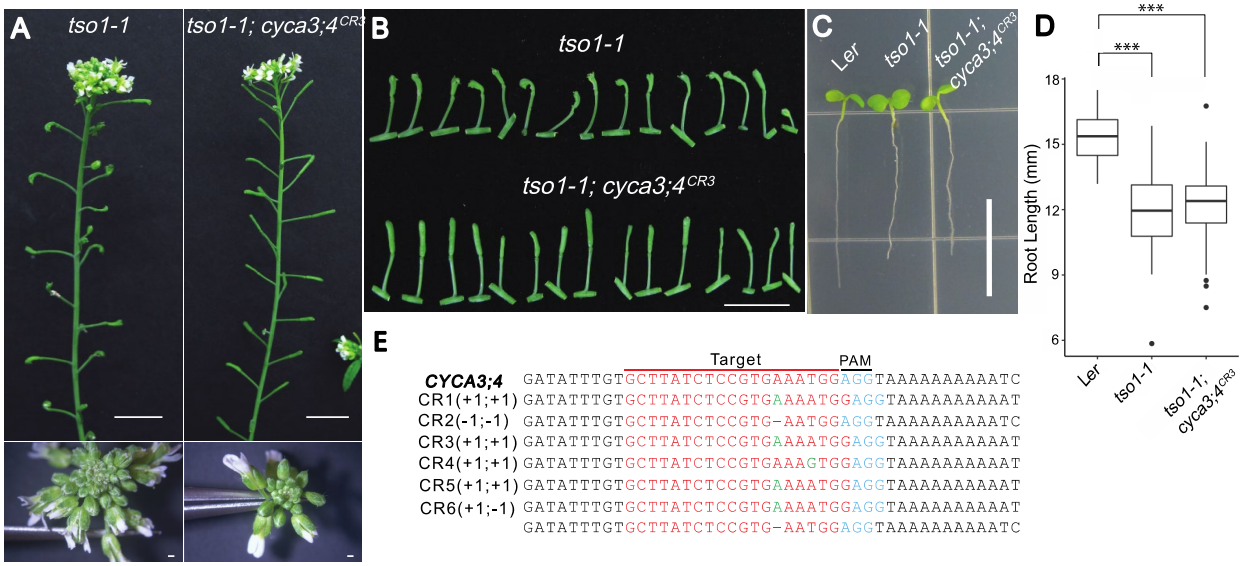

Figure 2.5 CRISPR/Cas9 knockouts of *CYCA3;4* suppress *tso1-1* shoot but not root defects. (A) Defects of *tso1-1* in fertility (top) and meristem fasciation (bottom) are suppressed by a CRISPR knockout mutation in *CYCA3;4*. (B) Comparing siliques of *tso1-1* with *tso1-1; cyca3;4*^{CR3}. While *tso1-1* carpels stay unfertilized and contain no seed, the *tso1-1; cyca3;4*^{CR3} form short siliques with a few seeds inside. (C) *tso1-1* mutants develop short roots in comparison to wild type (Ler). A *tso1-1; cyca3;4*^{CR3} double mutant has a root length similarly to *tso1-1*. (D) Quantification of root length in different genotypes. *** stands for $p<0.001$ (one-way ANOVA and Tukey's test). (E) CRISPR/CAS9-generated mutant alleles of *CYCA3;4.* Red font marks the seed RNA, green font highlights insertions, "-" and "+" indicate deletion and insertion respectively, and blue font marks PAM. Scale bars: 1cm in A (upper), B and C, 500µm in A (lower).

CRISPR/Cas9 directed knock-out of *CYCA3;4* allowed us to investigate if the *cyca3;4* mutations could suppress the *tso1-1* short root phenotype without worries of background mutations caused by the EMS mutagenesis. Both *tso1-1* and *tso1-1; cyca3;4*^{CR3} plants had similar root length, which is shorter than that of wild-type L*er* (Figure2.5 C and D), suggesting that mutations in *CYCA3;4* do not suppress *tso1-1's* short root phenotype. It remains to be determined if this tissue-specific suppression of

tso1-1 by the *cyca3;4* mutations is due to tissue-specific function of different members of the *CYCA3* family, which are known to exhibit different expression patterns (Takahashi *et al.*, 2010; Willems *et al.*, 2020).

2.2.3 *CYCA3;4* is mis-regulated in tso1-1 mutants

To understand the mechanism of *tso1* suppression by *cyca3;4*, we analyzed the expression of *CYCA3;4* in wild-type and *tso1-1*. A translational reporter of *CYCA3;4* (*pCYCA3;4-gCYCA3;4-GUS*) was constructed and transformed into plants heterozygous for *tso1-1.* Seven independent transgenic lines were analyzed. Reporter GUS expression was compared among the T_2 siblings from the same T_1 parent; these T_2 siblings are either *tso1-1* or wild type *(+/+ or tso1-1/+*). In the T_2 wild type inflorescences, light and even blue staining was observed in the young floral buds (Figure2.6 A and B). At floral stages 9-10, the locule of anthers show intense blue staining (white arrow in Figure2.6 A); at stages 10-12, intense staining occurs in ovules inside the gynoecium as well as stigma (see inset of Figure2.6 A). Therefore, the *CYCA3;4* expression is at the highest in actively dividing germ cells. In *tso1-1* mutant inflorescences, young floral buds showed significantly stronger GUS staining in young floral organ primordia and floral meristems (Figure2.6 C and D). In *tso1-1* plants with a strong phenotype including meristem fasciation and a lack of floral organ differentiation, strong and punctate staining were observed (Figure2.6 E and F). Since *tso1-1* mutants do not form well differentiated stamen or carpels, we do not see strong blue staining in gynoecium nor anthers. The sustained and stronger reporter GUS expression in the *tso1-1* young floral organs and meristems suggest two possible and not mutually exclusive possibilities. First, *TSO1* may repress the expression of

CYCA3;4 in young floral primordia to limit proliferation and encourage differentiation. A loss of *TSO1* resulted in over- and ectopic expression of *CYCA3;4*

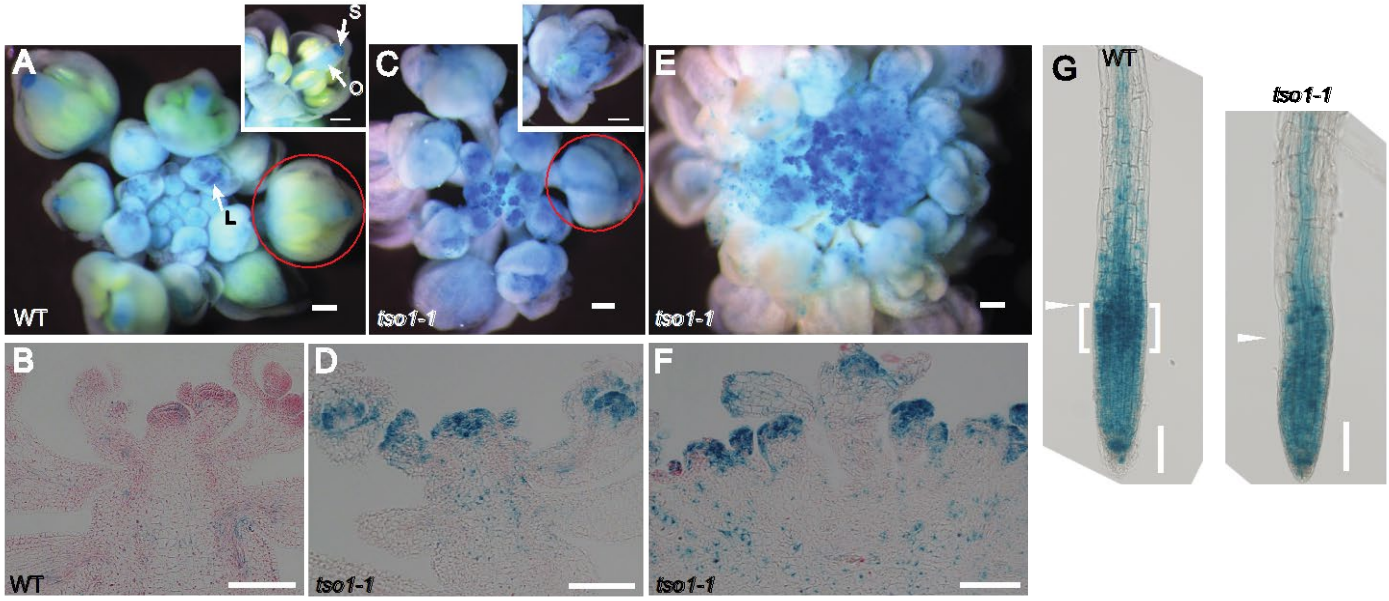

Figure 2.6 *pCYCA3;4::CYCA3;4-GUS* reporter expression in wild type and *tso1-1* inflorescences and roots.
(A) GUS reporter expression (blue) in an inflorescence of a wild type transgenic plant harboring *pCYCA3;4::CYCA3;4-GUS*. Inset shows a stage 11 flower. Arrows point to locule (L) of anther, stigma (S), and ovule (O). (B) A longitudinal section of the same wild type inflorescence in A. Eosin Y counterstain the tissues in pink. (C). GUS expression in an inflorescence of a *tso1-1* transgenic plant containing *pCYCA3;4::CYCA3;4-GUS*. Inset is a stage 11 flower. (D) A longitudinal section of the same *tso1-1* inflorescence shown in C with strong and patchy GUS staining throughout the young floral meristems and organ primordia. (E). GUS staining in a fasciated *tso1-1* inflorescence. Significantly more young floral meristems are formed and all strongly stained blue. (F). A longitudinal section of the same *tso1-1* inflorescence shown in E. (G) GUS staining of a 5 DPG root tip in wild type and *tso1-1*. Arrowheads indicate the upper boundary of RAM and brackets indicate a stronger GUS staining band at the most distal region of the RAM. Scale bars: 200μm in A, C and E, 100μm in B, D, F, and G.

and hence meristem over-proliferation and failure in floral organ differentiation. Alternatively, loss of *TSO1* may let to many cells that are unable to complete cell cycle and arrest at the G2/M or other cell cycle phases that express *CYCA3;4*. The partial suppression of the *tso1-1* phenotype by removing *CYCA3;4* function via mutations supports the first possibility.

We also compared the CYCA3;4 reporter expression in the roots. Consistent with previous published data (Willems *et al.*, 2020), the CYCA3;4-GUS fusion proteins are located in the meristematic zone and the transition zone in all cell layers (Figure2.6 G). In the elongation zone, CYCA3;4-GUS fusion is restricted in the stele. Similar to the wild-type, the CYCA3;4-GUS fusion proteins are also restricted to the same tissues in *tso1-1* roots (Figure2.6 G). However, the meristem zone is compressed in *tso1-1* root. Further, while the CYCA3;4-GUS proteins are more abundant near the transition zone in the wild-type root, CYCA3;4-GUS seems to more evenly distributed throughout the meristematic zone and lacks a strong staining band at the transition zone. In summary, *TSO1* does not seem to repress the expression of *CYCA3;4* in the root, but it may impact the spatial distribution of *CYCA3;4* due to *TSO1's* impact on root development (Wang *et al.*, 2018).

2.2.4 Overexpression of *CYCA3;4* weakly enhances the *tso1-3* fertility defect

As we revealed *CYCA3;4* mis-expression in *tso1-1,* we wondered about the possibility of over expression or ectopic expression of *CYCA3;4* in mediating the *tso1-1* mutant phenotype. We tested this possibility by overexpressing *CYCA3;4* in weak *tso1-3* mutants to see if over-expressed *CYCA3;4* enhances *tso1-3* phenotype. *pUBQ10::CYCA3;4* was introduced into *tso1-3/+* plants and the phenotype was compared among T2 sibling in three independent lines. There was no visible phenotypic difference between wild type plants with or without the *pUBQ10::CYCA3;4* transgene (Figure2.7 A and B). However, *tso1-3* plants containing the *pUBQ10::CYCA3;4* transgene showed smaller and more abnormal

siliques (Figure 4A, B). RT-qPCR showed 7-16 fold higher expression of *CYCA3;4* in three different *pUBQ10::CYCA3;4* transgenic lines (Figure2.7 C). We quantified and compared the number of seeds per silique in these three transgenic lines in comparison to *tso1-3;* two of the three *tso1-3* transgenic lines made fewer seeds per silique than the *tso1-3* control although the difference is small (Figure2.7 D). Therefore, overexpressing *CYCA3;4* enhances the fertility defect of *tso1-3* and overexpressed *CYCA3;4* may have contributed to the *tso1* mutant shoot phenotypes.

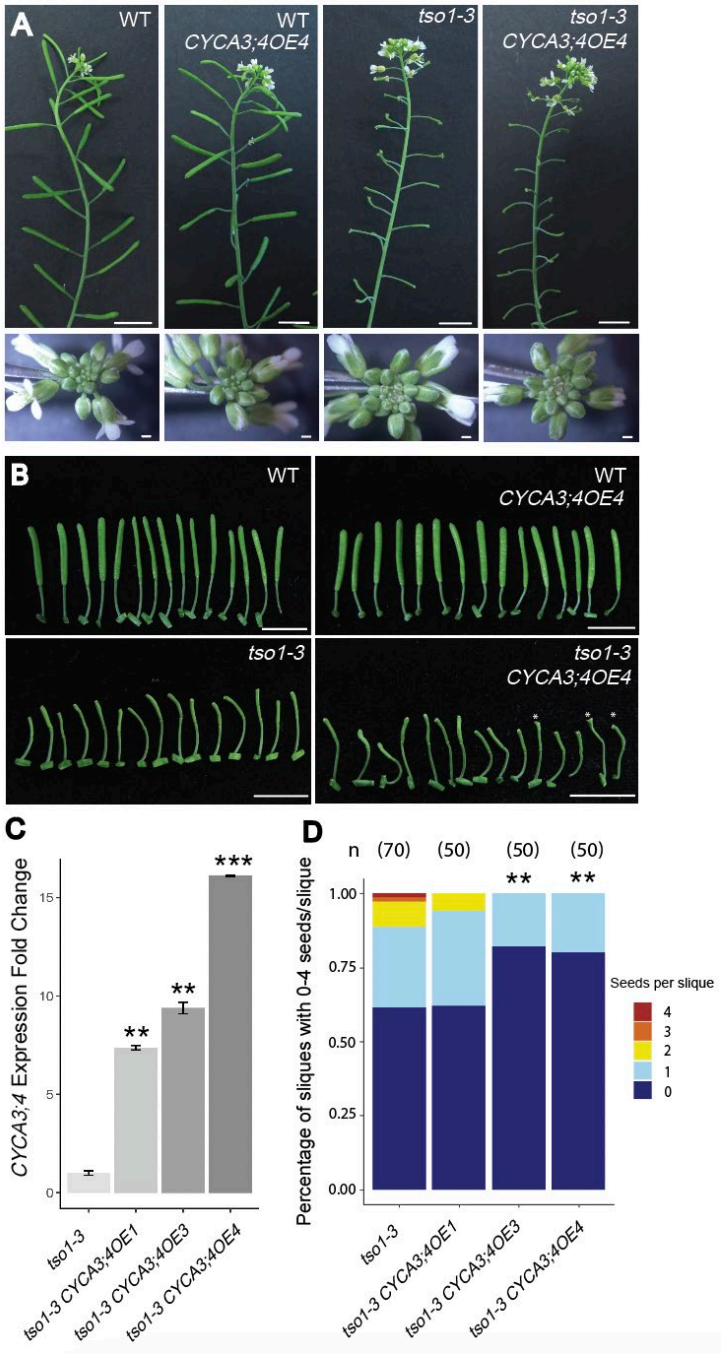

Figure 2.7 Overexpression of *CYCA3;4* enhances *tso1-3* fertility defects.
(A) Overexpression of *CYCA3;4* in *tso1-3* didn't significantly alter the morphology of SAM. (B) *tso1-3* plants with *CYCA3;4OE* have more unfertilized carpels due to severely abnormal carpels (marked by *). (C) RT-qPCR results showing higher expression levels of *CYCA3;4* in the three *CYCA3;4OE* transgenic lines. (D) *CYCA3;4OE* leads to poorer fertility in *tso1-3*. Y-axis indicates percentage of siliques with specific number of seeds. Numbers of siliques used for quantification are on top of the graph. **stands for $p<0.05$, ***stands for $p<0.001$ (One-way ANOVA and Tukey's test). Scale bars: 1cm in A (upper) and B, 500μm in A (lower).

2.2.5 A *TSO1-MYB3R-CYCA3;4* regulatory module in shoot meristem regulation

Previously, TSO1-MYB3R1 was found to encode a cell cycle regulatory module (Wang *et al.*, 2018). In SAM, TSO1 represses *MYB3R1* transcription to prevent G1-S transition and limit cell proliferation. At the G2-M cell cycle phases, however, TSO1 and MYB3R1 likely form a complex to promote G2-M gene expression and cytokinesis (Wang et al., 2018). We are curious about the role of *CYCA3;4* in the context of this *TSO1-MYB3R1* regulatory module. One hypothesis is that *TSO1* may repress *CYCA3;4* expression indirectly by repressing *MYB3R1* expression to prevent the G1-S transition. In *tso1-1*, ectopic *MYB3R1* leads to ectopic *CYCA3;4* expression which may cause over-proliferation of shoot meristem cells. In this hypothesis, *MYB3R1* may directly bind and activate *CYCA3;4*. We searched the Plant Cistrome Database containing the DAP-seq/ampDAP-seq data of *Arabidopsis* transcription factors (O'Malley *et al.*, 2016) and found a MYB3R1 binding peak in the promoter of *CYCA3;4* in the ampDAP-seq data, which shows in vitro-expressed-TF binding to PCR-amplified DNA fragments. Therefore, MYB3R1 can bind naked promoter region of *CYCA3;4* (Figure2.8 A). To further test this possibility, a transient dual-luciferase assay was subsequently performed in tobacco leaves testing the activity of *MYB3R1* on the *CYCA3;4* promoter driven LUC (Figure2.8 B). Compared with the control effector YFP, MYB3R1 caused higher luciferase activities even without fusion to the VP64 activation domain (Figure2.8 C, D). Combining with the observation that the *CYCA3;4* expression domain (Figure2.6) overlaps with that of *MYB3R1* (Wang *et al.*, 2018), our data support a direct and positive regulatory role of MYB3R1 for *CYCA3;4* expression.

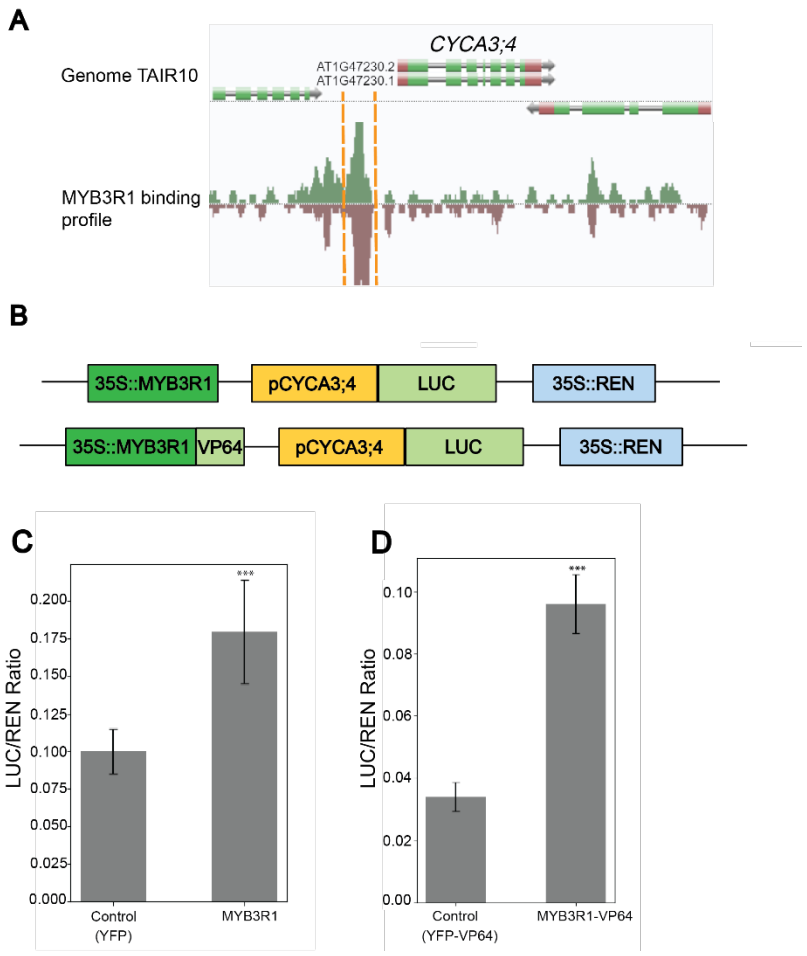

Figure 2.8 MYB3R1 can bind to the promoter of *CYCA3;4* and activates its transcription (A). ampDAP-Seq read abundance highlighting an MYB3R1 binding peak at the promoter of *CYCA3;4*, which is based on Plant Cistrome (O'Malley et al., 2016). (B) Diagram of the plasmid constructs used in the dual-luciferase assay. (C) and (D) Dual-luciferase assay results showing relative reporter expression of LUC/REN (Y-axis) in tobacco leaves. *** stands for $p<0.001$ (T-test, two-tailed).

2.3 Discussion

The plant DREAM/MMB complexes have been demonstrated to have an important impact on development, DNA damage response, and maintenance of methylations (Wang *et al.*, 2018; Simmons *et al.*, 2019, p. 1; Ning *et al.*, 2020; Lang *et al.*, 2021). Among the eight *Arabidopsis* homologs of animal LIN54, *Arabidopsis* TCX5 and

TCX6 were shown to act in plant DREAM complexes to preclude DNA hypermethylation and prevent excessive cell proliferation (Ning *et al.*, 2020). The function of SOL1 and SOL2 is required for efficient cell fate transition in stomata lineage, but they act oppositely to TSO1 in regulating the final division to produce the guard cells (Simmons *et al.*, 2019). Previously, we showed that the *TSO1-MYB3R1* module regulates proper development of SAM and RAM (Wang *et al.*, 2018). Despite the discovery of *MYB3R1* itself as a target of regulation by the *TSO1-MYB3R1* module, little is known about how this module, and by inference the DREAM/MMB, balances the cell division and differentiation at the shoot and root meristems. The finding of *CYCA3;4* as a target of the *TSO1-MYB3R1* regulatory module directly links this meristem regulatory module to cell cycle regulation and reveals the mechanism by which *TSO1-MYB3R1* may specifically regulate a member of the cyclin A family to control cell division rate at the shoot meristem.

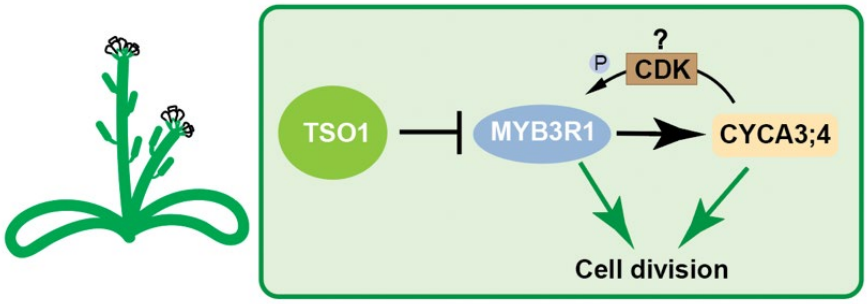

Figure 2.9 A regulatory module consisting of *TSO1*, *MYB3R1* and *CYCA3;4* regulates stem cell proliferation in *Arabidopsis* SAM.
TSO1 represses the expression of *MYB3R1,* and *MYB3R1* in turn promotes *CYCA3;4* expression. *CYCA3;4,* together with CDK, may activate MYB3R1 through phosphorylation, forming a feed-forward regulatory loop. Together, MYB3R1 and CYCA3;4 promote cell division. In wild type SAM, TSO1 limits cell division activity by repressing the expression of *MYB3R1* and indirectly *CYCA3;4.*

2.3.1 *CYCA3;4* is a unique *CYCA3*

In *Arabidopsis*, there are 50 putative cyclin genes in the genome (Nieuwland, Menges and Murray, 2007), which can be classified into eight classes (*CYCA1-3*, *CYCB1-3*, *CYCC*, *CYCD1-7*, *CYCH*, *CYCL*, *CYCP1-4* and *CYCT*) plus 3 additional unclassified cyclins (*CYCJ18*, *SOLODANCERS* and *CYL1*) (Menges *et al.*, 2005). Among the A-type cyclins, *CYCA3s* were believed to govern the G1-S transition, a function that resembles the E-type cyclin in animals (Yu *et al.*, 2003). The expression profiles of the four *CYCA3* cyclins in *Arabidopsis* vary greatly, suggesting potentially diverse functions. For instance, *CYCA3;1* and *CYCA3;2* peak in the S phase while *CYCA3;4* was found to have a constant expression across all cell cycle phases in the synchronized *Arabidopsis* MM2d cell line and roots (Takahashi *et al.*, 2010). However, *CYCA3;4* proteins accumulate mainly in the G_2/M phase in the root (Willems *et al.*, 2020). *CYCA3;3* is a meiosis-specific cyclin and not expressed in somatic cells (Bulankova *et al.*, 2013).

A prior study aimed at identifying substrates of the Anaphase Promoting Complex/Cyclosome (APC/$C^{CCS52A2}$) isolated genetic suppressors of *ccs52a2-1*, which is defective in the activator subunit CCS52A2 of APC/$C^{CCS52A2}$. A mutation in *CYCA3;4A* (*cyca3;4-1)* was identified that partially suppressed *ccs52a2-1*'s short root phenotype. Interestingly, single knockouts of *CYCA3;4* in *Arabidopsis*, including *cyca3;4-2* and *cyca3;4-3* caused by T-DNA insertions, caused no obvious phenotype. Therefore, functional redundancy may still exist among family members (Willems et al., 2020). However, mutations in *CYCA3;1 and CYCA3;2* did not suppress *ccs52a2-1*. Thus *CYCA3;4* is the main degradation target of APC/$C^{CCS52A2}$.

Our genetic screen also identified a single mutation in *CYCA3;4* as the suppressor of *tso1-1*. As our mutagenesis screen of *tso1-1* is likely saturated due to the isolation of 32 *myb3r1* mutant alleles as the suppressors of *tso1-1* (Wang *et al.*, 2018), a lack of suppressor mutations in other *CYCA3* genes suggests that *CYCA3;4* is likely the only *CYCA3* regulated by the *TSO1-MYB3R1* module. In support of this, *CYCA3;4* is the only *CYCA3*s in the target gene list of MYB3R1 in the ampDAP-seq data base (O'Malley *et al.*, 2016), and *CYCA3;4* expression is distinct from *CYCA3;1*, *CYCA3;2*, and *CYCA3;3* (Takahashi *et al.*, 2010; Willems *et al.*, 2020). Therefore, *CYCA3;4* could be the only or the major *CYCA3* gene involved in the *TSO1-MYB3R1* regulatory module in the shoot meristem.

2.3.2 Potential mechanisms of *CYCA3;4* in meristem regulation

Cyclins normally function by binding and activating cyclin-dependent kinases (CDKs) as well as helping specify substrates (Kõivomägi *et al.*, 2011; Tank and Thaker, 2011; Harashima and Schnittger, 2012). Earlier research showed that the *Arabidopsis* CYCA3;4 can bind CDKA;1 (Van Leene *et al.*, 2010) suggesting CDKA;1 a likely partner of CYCA3;4 in meristem regulation. Previously, when *CYCA3;4* was overexpressed in the wild type *Arabidopsis* seedlings, several phosphorylation targets including RBR1 were shown to be hyperphosphorylated (Willems *et al.*, 2020); MYB3R1 was not among the phosphorylation targets in the study that uses young seedlings. Nevertheless, MYB3R1 could be a phosphorylation target of CYCA3;4/CDKA;1 in shoot and root meristems as MYB3Rs need to be phosphorylated in order to be active (Araki *et al.*, 2004; Haga *et al.*, 2007). A phosphomimic MYB3R1 (presumably over-active MYB3R1) was previously shown

to enhance the *tso1-3* shoot phenotype (Wang *et al.*, 2018). The phenotype of the *CYCA3;4* overexpression plants resembled the phenotype of the phosphomimic MYB3R1 plants, that could possibly result from the over-activation of *MYB3R1* by the increased CYCA3;4/CDKA;1 complex.

Based on our findings as well as prior reports, we propose a model (Fig. 6), in which *TSO1* may act at the G1-S phase to prevent *MYB3R1* expression and cell proliferation in the SAM. In *tso1-1* mutants, when *TSO1* activity is lost, *MYB3R1* is over- and constitutively expressed leading to constitutive expression of *CYCA3;4*. This increased *CYCA3;4* subsequently promotes cell division cycle by phosphorylating RBR1, MYB3R1 and other substrates, causing over-proliferation of stem cells in the *tso1-1* SAM. The model suggests a possible positive feedback loop between MYB3R1 and CYCA3;4 through phosphorylation. Unfortunately, we failed to purify the stable CYCA3;4/CDKA;1 complex that could be used for the kinase assay of MYB3R1.

Interestingly, the binding of MYB3R1 to the *CYCA3;4* promoter is observed in the ampDAP-seq that tests TF binding to PCR-amplified DNA fragment, but not in the DAP-seq that tests binding to genomic DNA fragments retaining 5-methylcytosines. Hence, the binding of MYB3R1 to the *CYCA3;4* promoter might be sensitive to cytosine methylation and likely tissue- and cell cycle phase-specific.

2.4 Methods

2.4.1 Plant materials and growth conditions

Plants were grown on soil (Sungrow) under a 16-h light/8-h dark cycle at 20℃. All mutants used are in Landsberg *erecta* (L*er*) background. *tso1-1*, *tso1-3,* and plants

heterozygous for *tso1-1* or *tso1-3* (*tso1-1 +/+ sup-5* and *tso1-3 +/ + sup-5*) were described previously (Liu, Running and Meyerowitz, 1997; Hauser, Villanueva and Gasser, 1998; Sijacic, Wang and Liu, 2011; Wang *et al.*, 2018). *cyca3;4-4* (A144) was isolated from an EMS mutagenesis screen of *tso1-1; 35S::TSO1-GR* (Wang *et al.*, 2018).

2.4.2 Constructs and transformation

All constructs were transformed through floral dip using *Agrobacterium* strain GV3101. All sequences were cloned from L*er*. All relevant primers are listed in Table S1.

For the complementation test construct, genomic sequence of *CYCA3;4* (from the start of the 5'UTR to the end of the 3'UTR plus ~1.4kb upstream of the 5'UTR) was PCR amplified with primers (Table S1), cloned into pCR8/GW/TOPO, and LR-recombined into pMDC99 (Curtis and Grossniklaus, 2003).

For the CRISPR/Cas9 construct targeting *CYCA3;4*, the crRNA was designed using the website crispr.dbcls.jp/. Two 19-nt guide sequences (Table S1) were chosen as they had no off-target sites. crRNA1 and crRNA2 respectively target the first few nucleotides and the last few nucleotides of the first exon. To introduce the two crRNAs into the pHEE401E vector (Wang *et al.*, 2015), cloning PCR was carried out using the pCBT-DT1T2 vector as the template and the PCR product containing the two crRNAs was introduced into pHEE401E via Gibson assembly (Gibson *et al.*, 2009). The construct was transformed into *tso1-1; 35S::TSO1-GR* plants. Only crRNA2 was able to generate successful knock-out of *CYCA3;4*. No DEX was applied when analyzing the phenotype of the transgenic plants.

The *pCYCA3;4* (~1.4kb) and the genomic sequence of *CYCA3;4* (from the start of 5'UTR to the end of the coding region) were cloned into pCR8/GW/TOPO and recombined into pMDC162 (Curtis and Grossniklaus, 2003) to make the *pCYCA3;4::CYCA3;4-GUS* translational fusion. The construct was transformed into *tso1-1 +/+ sup-5* plants. Seven independent transgenic lines were analyzed. GUS expression pattern was compared between wild type and *tso1-1* T2 sibling plants derived from the same T_1 parent (*tso1-1 +/+ sup5)*.

To overexpress *CYCA3;4*, the *Arabidopsis UBQ10* promoter was cloned from the JH23 vector (Zhou *et al.*, 2021) and used to drive full length cDNA of *CYCA3;4* (*pUBQ10::CYCA3;4*). *pUBQ10::CYCA3;4* was first cloned into pCR8/GW/TOPO through Gibson assembly and LR recombined into pEarleyGate301 (Earley *et al.*, 2006). *pUBQ10::CYCA3;4* was introduced into agrobacterium GV3101 and used to floral dip *tso1-3 +/+ sup-5* plants. T_2 plants from three independent transgenic lines were analyzed. Seeds in the 6^{th} – 15^{th} siliques on the main shoot were quantified.

For dual luciferase assay, *pCYCA3;4* (~1.4kb) was cloned into LEI01, LEI02, LEI03 and LEI04 (Zhou *et al.*, 2021) at NotI and BamHI. The CDS of *MYB3R1* was amplified and cloned into *pCYCA3;4*-containing LEI01 and LEI02 at EcoRI and AscI. These four constructs were then used in LR reactions to transfer the insertions into the vector pLAH-LARm (Taylor-Teeples *et al.*, 2015) to make *35S::MYB3R1-pCYCA3;4::LUC-35S::REN*, *35S::MYB3R1-VP64-pCYCA3;4::LUC-35S::REN*, *35S::Citrine-pCYCA3;4::LUC-35S::REN*, *35S::Citrine-VP64-and pCYCA3;4::LUC-35S::REN*.

We noticed a mis-annotation of *CYCA3;4* based on Col-0 and L*er* cDNA sequences, where the first 3 nucleotides in the 3rd exon should be in the intron.

2.4.3 Mapping by sequencing

The mapping population was created by crossing *A144* (in the *tso1-1; 35S::TSO1-GR* background) with the parent plant (+/+, *tso1-1; 35S::TSO1-GR)*. Leaf tissues were collected and pooled from 34 suppressed F2 plants and 50 unsuppressed F2 plants, respectively. Genomic DNAs were extracted using the NucleoSpin Plant II Midi Kit (Macherey-Nagel) and then sent for Illumina sequencing (PE-150). The sequencing depth of the suppressed plants was 202 folds. The sequencing depth of the unsuppressed group was 95 folds. The SIMPLE pipeline (Wachsman *et al.*, 2017) was employed for mapping A144 with default settings.

2.4.4 Root assay

The seeds were sterilized with 70% ethanol and 10% bleach and then kept in water at 4°C in the dark for 2 days, after which the seeds were planted on ½ MS (RPI) medium and allowed to germinate under dim light environment for 2 days. Once germinated, they were transferred to the growth chamber. 5-DPG (Days Post Germination) roots were used for quantification.

2.4.5 GUS staining and Sectioning

Inflorescences or 5-DPG seedlings were soaked in 90% acetone for 20min at room temperature, followed by three washes of staining buffer [0.2% Triton X-100, 50mM NaHPO4 Buffer (pH7.2), 2mM Potassium Ferrocyanide, 2mM Potassium Ferricyanide]. They were then stained in a buffer with 2mM X-Gluc for 3 to 3.5 hours. Tissues were cleared with ethanol series (20%, 35%, 50%) and then stored in 70% ethanol at 4°C before imaging. Subsequently, tissues were embedded and

sectioned based on a published protocol (Hollender *et al.*, 2012). Imaging was performed with Zeiss LSM980 and Zeiss Stemi SV 6.

2.4.6 Dual-luciferase assay

Dual-luciferase assay were carried out according to the protocol described previously (Taylor-Teeples *et al.*, 2015; Zhan *et al.*, 2018; Zhou *et al.*, 2021).

2.4.7 RNA extraction and RT-qPCR experiments

Arabidopsis SAMs were collected for RNA extraction using RNeasy Mini Kit (Qiagen). RNA samples were cleaned with DNase I. cDNAs were synthesized using RevertAid First Strand cDNA Synthesis Kit (ThermoFisher). RT-qPCR experiments were performed on the Bio-rad CFX 96 machine with PowerUp™ SYBR® Green Master Mix (Thermo Fisher). Three biological replicates were conducted for the RT-qPCR with three technical replicates. The *TIP41(AT4G34270)* gene was used as the internal control.

Chapter 3: Single cell RNA sequencing revealed possible causes of *tso1-1* short root phenotype

3.1 Introduction

As one of the most important organs of vascular plants, roots play essential roles in up-taking water and nutrients as well as anchoring the plants to the ground (Macdonald and Stevens, 2019). Sitting at the tip of the root is a tissue called the root apical meristem (RAM). The RAM is responsible for generating new cells and maintaining pluripotent stem cells at the same time. Sitting at the tip of the RAM are a small group of cells named the quiescent center (QC) (Figure1.2 B). The QC contains pluripotent stem cells that give birth to the initials/stem cells for each layer of the root (Figure1.2 B). The maintenance of QC is essential for root growth; the root growth and the RAM size are greatly reduced in the mutant of genes that specify QC identity (Aida *et al.*, 2004).

The *Arabidopsis* transcription factor *TSO1* has been shown to function in the root development. The *tso1-1* mutant produces much shorter root when compared to the wild type (Wang *et al.*, 2018). Closer examination revealed that this phenotype was due to the shrinkage of the RAM. Mutations in the *TSO1* target gene *MYB3R1* suppressed the short root phenotype of *tso1-1*, and the double mutant *tso1-1; myb3r1* showed normal root length. *MYB3R1* was found overexpressed in the *tso1-1* root. These data suggest that the overexpression of *MYB3R1* mediates the short root phenotype in the *tso1-1* mutant. Nevertheless, no other *TSO1* targets have been identified in the root. Little is known about the molecular mechanisms of how *TSO1* regulates root development.

The single-cell RNA sequencing (scRNA-seq) technique is becoming a popular tool for analyzing plant gene expression. Before the scRNA-seq, the bulk RNA sequencing was often used to examine gene expression within a mixture of different cell types. With bulk RNA-seq, it was hard to detect changes in gene expression for genes with cell type-specific expression, in particular those expressed in tissues like root QC (pluripotent stem cell), which consists of only a few cells. The scRNA-seq, on the other hand, allows analysis of gene expression at single cell level, revealing new information on gene expression and regulation (Shaw, Tian and Xu, 2021). Though scRNA-seq is only in its early stages in plant sciences and there are still many challenges, it has already demonstrated its power in revealing gene expression heterogeneity between cells (Shaw, Tian and Xu, 2021). The scRNA-seq has been applied to investigating developmental trajectories, identifying new developmental regulators as well as comparing cell differentiation pathways of cell identity mutants (Ryu *et al.*, 2019; Liu *et al.*, 2020; Zhang, Chen and Wang, 2021; Shahan *et al.*, 2022). It has also been used in rice to identify transcription factor targets (Xie *et al.*, 2020). In addition, the early-stage single-cell research provides useful tissue-references for others who are interested in conducting scRNA-seq. The construction of several organ-scale scRNA-seq references/gene expression atlases greatly simplifies the process of scRNA-seq data analysis (Zhang, Chen and Wang, 2021; Shahan *et al.*, 2022). These references are based on both established experimental cell markers as well as cell markers identified through bioinformatic analysis of scRNA-seq data. With these references, specific tissues and cells can be clearly identified based on their characteristic gene expression signatures. The information provided by

these references can be projected onto any scRNA-seq dataset to identify specific cell types or developmental stages within that dataset.

The availability of scRNA-seq for plants provides a great opportunity for the study of *TSO1*, especially for understanding the short root phenotype of *tso1-1*. The only difference observed between *tso1-1* root and wild type is the reduction of the RAM size, indicated by the reduced number of cortex cells (Wang *et al.*, 2018). The limited knowledge about *tso1-1* root makes it hard to learn the molecular mechanisms behind *TSO1*'s function. However, with the scRNA-seq, we can determine if there's any change in the cell identity, the ratio of each cell type, and the gene expression pattern within specific cell types in the *tso1-1* mutant root all at once.

By comparing the scRNA-seq data of *tso1-1* and wild type roots, changes in the percentage of specific cell types were observed and several potential *TSO1* target genes were found. Reduction of the percentage of vascular cells were seen in the *tso1-1* mutant, indicating defects in vasculature development. Meanwhile, the potential *TSO1* target genes can be divided into three categories. The first category is the plant DREAM complex components, including *TSO1* itself. Increase of *TSO1*, *ALY1* and *MSI2* expression was seen in the *tso1-1* root, which suggests that *TSO1* regulates the expression of potential plant DREAM complex components to balance cell proliferation and cell differentiation in the root. The second category is the *HD-ZIP III* family. There are five members of the *HD-ZIP III* family: *PHABULOSA* (*PHB*), *PHAVOLUTA* (*PHV*), *REVOLUTA* (*REV*), *CORONA* (*CRN*)/*ATHB15* and *ATHB8*. These genes are known as regulators of vascular patterning in the root: high expression levels of the *HD-ZIP III* genes lead to metaxylem formation while low

expression levels of *HD-ZIP III*s lead to protoxylem formation (Carlsbecker *et al.*, 2010). More detailed descriptions of the *HD-ZIP III* family can be found in Chapter 1 of this dissertation. We found that the expression of *HD-ZIP III* genes is increased mainly in the vasculature of *tso1-1*. Two of the *HD-ZIP III*s (*PHB* and *PHV*) are ectopically expressed in the *tso1-1* metaxylem cells. Moreover, one of the *PHB* direct target, *IPT7*, was also found overexpressed in the metaxylem in *tso1-1*. *IPT7* falls into the third category of potential *TSO1* target genes, consisting of the cytokinin biosynthesis genes. Four cytokinin biosynthesis genes including *IPT7*, *IPT9*, *LOG1* and *LOG8* showed increased expression in the *tso1-1* root. Among them, the *LOG1* was specifically overexpressed in the endodermis cells while elevated expression of *IPT9* and *LOG8* were seen mainly in the QC.

Overall, these findings suggest that *TSO1* is involved in the negative regulation of cytokinin biosynthesis either by repressing the expression of *HD-ZIP III* genes in the vascular cells or by unknown mechanisms in other tissues like the endodermis and QC. It helps to explain the short root phenotype of *tso1-1* since applying exogenous cytokinin to *Arabidopsis* causes similar short root phenotype (Dello Ioio *et al.*, 2007). The increased production of cytokinin may mediate the *tso1-1* short root phenotype.

This project is a collaborative project between me and two other scientists. The sample preparation for scRNA-seq, Illumina sequencing and raw sequencing file processing (using Cell Ranger) were carried out by Dr. Rachel Shahan in Dr. Philip Benfey's lab at the Duke University. The global data analysis (protoplasting-induced gene removal, label transfer from reference and data integration) was performed by Muzi Li, a graduate student in Dr. Zhongchi Liu's lab at the University of Maryland –

College Park. The figures shown in this dissertation were generated by the dissertation author using Muzi Li's R script.

3.2 Results

3.2.1 Single cell transcriptomes revealed reduced cell number in the vasculature of *tso1-1* mutant root

To understand how *TSO1* regulates root development, comparative single cell transcriptome was conducted to identify differentially expressed genes in *tso1-1* and wild type (L*er*) roots. The roots of *tso1-1* and wild type (0.5cm from the tip, 5DPG) were collected for scRNA-seq (Figure 3.1 A). Two biological replicates were harvested for each genotype. The roots were then treated with enzymes to isolate the protoplasts/single cells. This step is required for the droplet-based scRNA-seq (10X Genomics) used in this study. After protoplasting, the samples were loaded onto microfluid chips (10X Genomics) to capture either 5,000 or 10,000 cells/sample. Barcoding of the cells were carried out with a Chromium Controller (10X Genomics). After reverse transcription and Illumina library preparation, the samples were sequenced with a Novaseq 6000 instrument (Illumina). The processing and analysis for our scRNA-seq datasets were summarized in Figure3.1 B. The raw scRNA-seq data were first processed by Cell Ranger to generate FASTQ files. Then the protoplasting-induced genes were removed using Seurat (Satija *et al.*, 2015). A root cell type reference (primary root gene expression atlas) was used to identify different cell types in our scRNA-seq datasets. This organ-scale reference was generated based on the combination of established experimental cell type markers, previous published

Arabidopsis root scRNA-seq datasets and an integration of 110,427 wild type *Arabidopsis* root scRNA-seq data. It includes 14 root cell types and 7 developmental stages (Denyer *et al.*, 2019; Ryu *et al.*, 2019; Shahan *et al.*, 2022). Using the label transfer function in Seurat (Satija *et al.*, 2015), the primary root gene expression atlas was projected to our scRNA-seq data to identify clusters of cells belonging to one of the fourteen cell types.

Combining the two biological replicates, about 27,000 cells from the wild type roots and 10,000 cells from *tso1-1* roots were captured (Table 3.1). The number of cells from the *tso1-1* roots is about 1/3 of the wild type, which is not surprising given past experiences that different mutant roots always yielded fewer cells than WT (Shahan

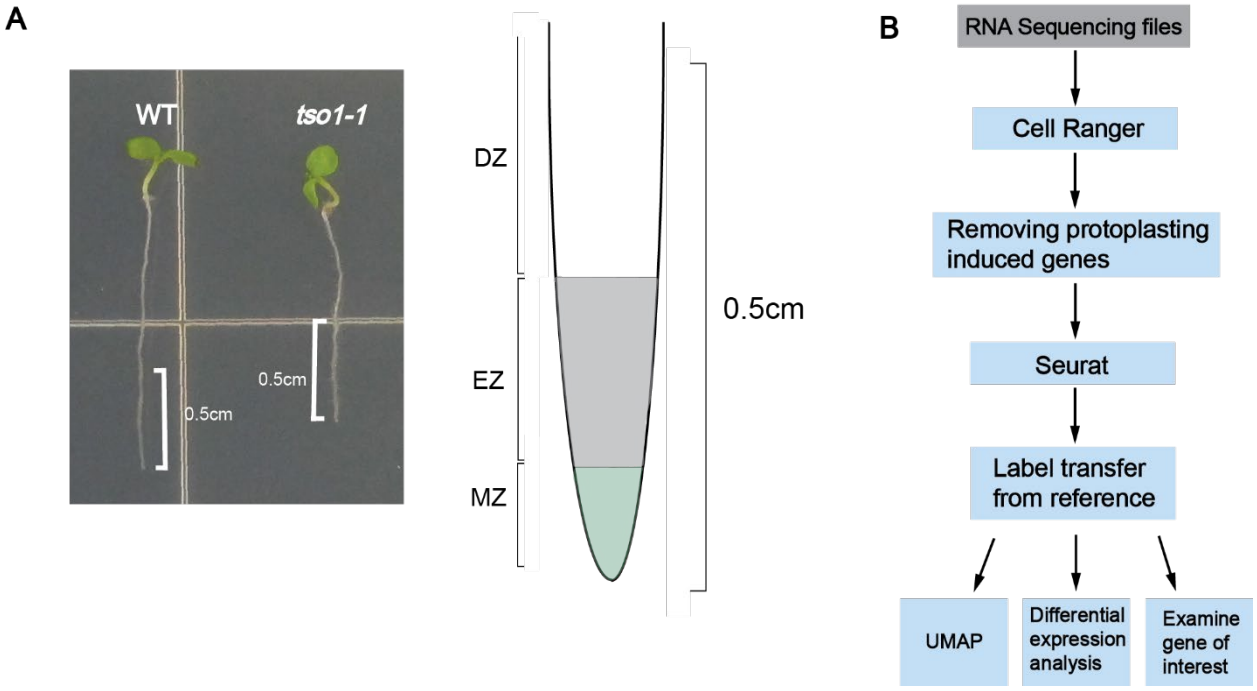

Figure 3.1 The pipeline of single cell data analysis.
(A) Photo and diagram showing the samples taken for scRNA-seq. The roots were harvested on 5DPG and 0.5cm was taken from the tip for protoplasting. The length covered three zones of both WT roots and *tso1-1* roots. MZ: meristematic zone, EZ: elongation zone, DZ: differentiation zone. (B) The analysis pipeline used in this study.

et al., 2022). After the label transfer, all 14 cell types were identified in wild type and *tso1-1* roots (Figure3.2 A), suggesting that the short root phenotype of *tso1-1* is probably not caused by missing certain cell types.

Though there was no change in cell identities observed in *tso1-1*, differences were observed in the percentage of a specific cell type among the total cells examined. In particular, the percentage of several vascular cell types were reduced in *tso1-1* when compared with WT (Figure3.2 D). The affected vascular cell types include protoxylem, metaxylem, procambium, metaphloem and companion cell, phloem pole pericycle and xylem pole pericycle. The result suggests that the short root phenotype of *tso1-1* might be caused by defects in vasculature development.

In order to compare the gene expression patterns in wild type and *tso1-1* mutant, the scRNA-seq data of wild type and *tso1-1* need to be combined and normalized (integration) by Seurat (Satija *et al.*, 2015). After the integration, known cell type markers were examined to evaluate the quality of the label transfer and integration (Figure3.2 C). All markers showed expression in the corresponding cell types, suggesting that the label transfer and integration were successful. The data can be used for further gene expression comparison.

Sample name	CellType	Cell number	Percentage(%)	Sample name	CellType	Cell number	Percentage(%)
WT_1	Atrichoblast	1494	12.11	WT_2	Atrichoblast	1543	11.33
WT_1	Columella	719	5.83	WT_2	Columella	666	4.89
WT_1	Cortex	2081	16.87	WT_2	Cortex	2171	15.94
WT_1	Endodermis	1614	13.08	WT_2	Endodermis	1785	13.11
WT_1	Lateral Root Cap	1829	14.82	WT_2	Lateral Root Cap	1997	14.67
WT_1	Metaphloem & Companion Cell	194	1.57	WT_2	Metaphloem & Companion Cell	188	1.38
WT_1	Metaxylem	153	1.24	WT_2	Metaxylem	152	1.12
WT_1	Phloem Pole Pericycle	340	2.76	WT_2	Phloem Pole Pericycle	358	2.63
WT_1	Procambium	559	4.53	WT_2	Procambium	559	4.11
WT_1	Protophloem	36	0.29	WT_2	Protophloem	69	0.51
WT_1	Protoxylem	242	1.96	WT_2	Protoxylem	226	1.66
WT_1	Quiescent Center	16	0.13	WT_2	Quiescent Center	23	0.17
WT_1	Trichoblast	2182	17.69	WT_2	Trichoblast	2973	21.83
WT_1	Xylem Pole Pericycle	879	7.12	WT_2	Xylem Pole Pericycle	906	6.65
tso1-1_1	Atrichoblast	903	18.29	*tso1-1_2*	Atrichoblast	510	11.03
tso1-1_1	Columella	562	11.39	*tso1-1_2*	Columella	517	11.18
tso1-1_1	Cortex	830	16.82	*tso1-1_2*	Cortex	632	13.67
tso1-1_1	Endodermis	426	8.63	*tso1-1_2*	Endodermis	560	12.11
tso1-1_1	Lateral Root Cap	955	19.35	*tso1-1_2*	Lateral Root Cap	1168	25.26
tso1-1_1	Metaphloem & Companion Cell	7	0.14	*tso1-1_2*	Metaphloem & Companion Cell	23	0.50
tso1-1_1	Metaxylem	6	0.12	*tso1-1_2*	Metaxylem	33	0.71
tso1-1_1	Phloem Pole Pericycle	12	0.24	*tso1-1_2*	Phloem Pole Pericycle	44	0.95
tso1-1_1	Procambium	77	1.56	*tso1-1_2*	Procambium	111	2.40
tso1-1_1	Protophloem	NA	NA	*tso1-1_2*	Protophloem	15	0.32
tso1-1_1	Protoxylem	9	0.18	*tso1-1_2*	Protoxylem	21	0.45
tso1-1_1	Quiescent Center	3	0.06	*tso1-1_2*	Quiescent Center	4	0.09
tso1-1_1	Trichoblast	1035	20.97	*tso1-1_2*	Trichoblast	775	16.76
tso1-1_1	Xylem Pole Pericycle	111	2.25	*tso1-1_2*	Xylem Pole Pericycle	211	4.56

Table3.1: Number of cells in each cell type and percentage of cells in a specific cell type over all cells in a sequenced sample.
Two biological replicates were collected and sequenced for each genotype: WT_1, WT_2 for wild type; *tso1-1_1* and *tso1-1_2* for *tso1-1* mutant.

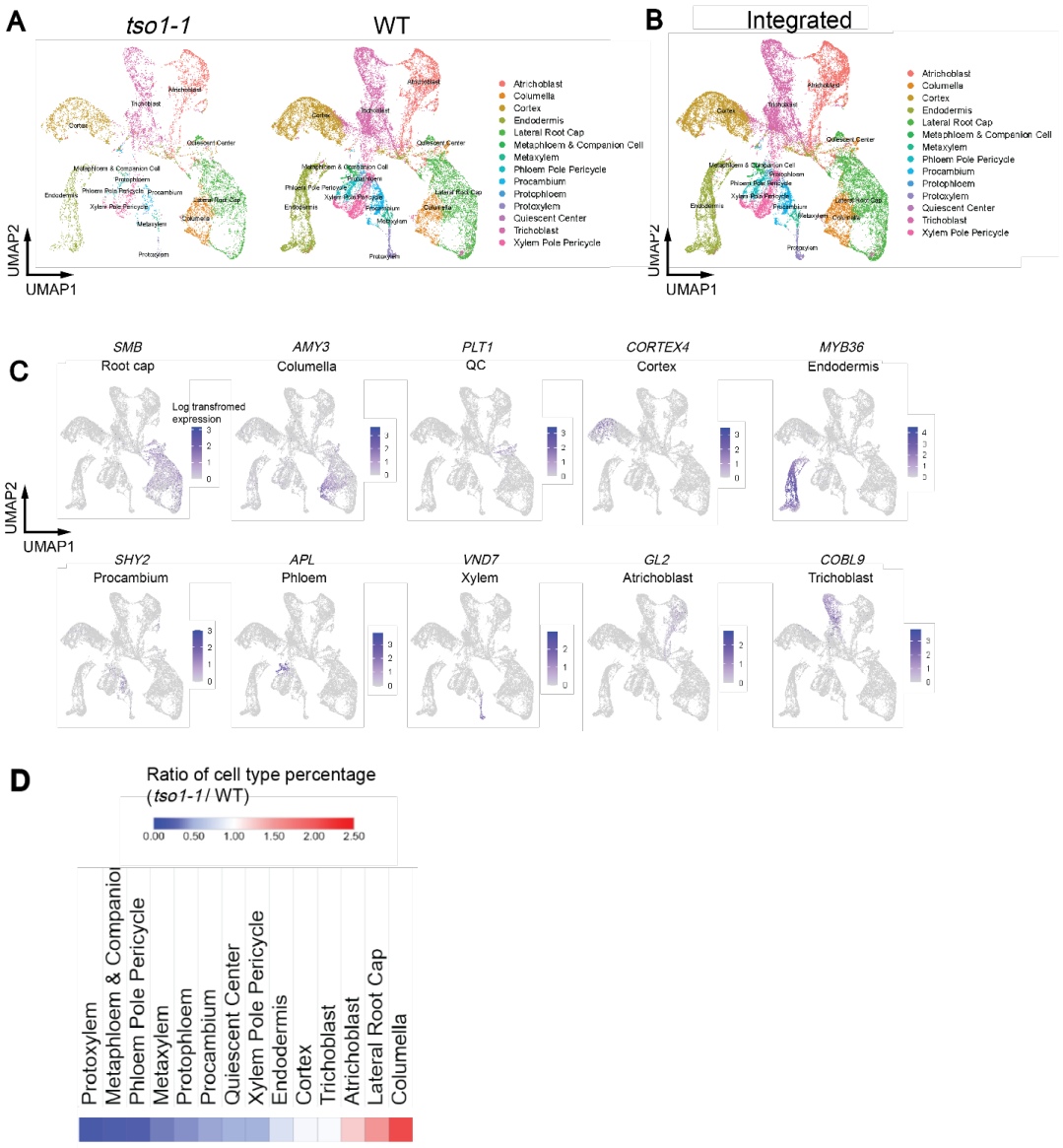

Figure 3.2: The single cell transcriptome analysis suggests that the percentage of vasculature cells is reduced in *tso1-1* root.
(A) UMAP showing the cell types of *tso1-1* and WT (Ler) roots. Each dot represents a single cell, and fourteen different cell types are marked by different colors. Cells belonging to the same cell type are clustered together. All fourteen cell types are found in the *tso1-1* root despite fewer total cells in the *tso1-1* root sample. (B) UMAP showing integrated wild type and *tso1-1* root single cell sequencing data. Normalization and scale were carried out using Seurat. (C) Feature plots (integrated) showing expression of known cell type marker genes. The name of the gene and cell type were labeled on the top of each plot. The scale shows log (log2) transformed normalized expression for corresponding gene. (D) A heatmap showing the ratio of cell type percentage between *tso1-1* and WT. The cell type percentage is the percentage of cells in a specific cell type over all cells in a genotype. The percentage of vascular tissues (protoxylem, metaxylem, protophloem, metaphloem and companion cell, phloem pole pericycle, xylem pole pericycle and procambium) is reduced in *tso1-1* root.

3.2.2 *TSO1* is ectopic and overexpressed in the *tso1-1* mutant root

Differentially expressed genes between WT and *tso1-1* were examined for all cell types. Surprisingly, increased *TSO1* expression was observed in nearly all cell types (Figure3.3 A). Specifically, *TSO1* is ectopically expressed in atrichoblast, columella, lateral root cap, cortex, endodermis, protoxylem, metaxylem, protophloem, metaphloem and companion cell, procambium, phleom pole pericycle, xylem pole pericycle and QC (Figure3.3 B). The increased expression of *TSO1* suggests that *TSO1* or the *TSO1*-containing plant DREAM complex represses the expression of *TSO1* in almost all wild type root cell types.

As a potential member of the plant DREAM complex, altered *TSO1* expression revealed above may affect DREAM complex activity. As DREAM complex is also involved in regulating the expression of DREAM complex components (Wang *et al.*, 2018; Iness *et al.*, 2019), we examined gene expression patterns of the plant DREAM components (Figure3.3). No significant difference was observed for most of the DREAM components (Figure3.3 A). Surprisingly, one of the previously characterized *TSO1* regulatory targets, *MYB3R1*, did not show any change in its expression pattern (Figure 3.3 C), even though *MYB3R1* was shown to be overexpressed in both *tso1-1* shoot and root (Wang *et al.*, 2018). Among the single cells captured in our study, very few cells express *MYB3R1* (Figure 3.3 C), which may explain why *MYB3R1* did not show significant expression difference due to too small number of cells. Similarly, very few cells express another *TSO1* target, *CYCA3;4* (Figure 3.3 D) described in chapter 2. Due to the small number of cells expressing these genes, statistically significant changes of gene expression may be difficult to detect. Increasing the total

number of cells in scRNA-seq may better enable us to examine *MYB3R1* and *CYCA3;4* expression.

Besides *TSO1*, two core DREAM components, *ALY1* and *MSI2*, are ectopically expressed in the *tso1-1* QC cells (Figure 3.3 E and F). *ALY1* and *MSI2* are homologs of the mammalian DREAM complex core component LIN9 and RBBP4 respectively (Table1.1). In addition, in *tso1-1* root, more cells expressed *MSI2* in metaxylem and xylem pole pericycle (Figure3.3 F), and more cells expressed *ALY1* in columella. Therefore, *TSO1* may regulate the expression of some potential plant DREAM

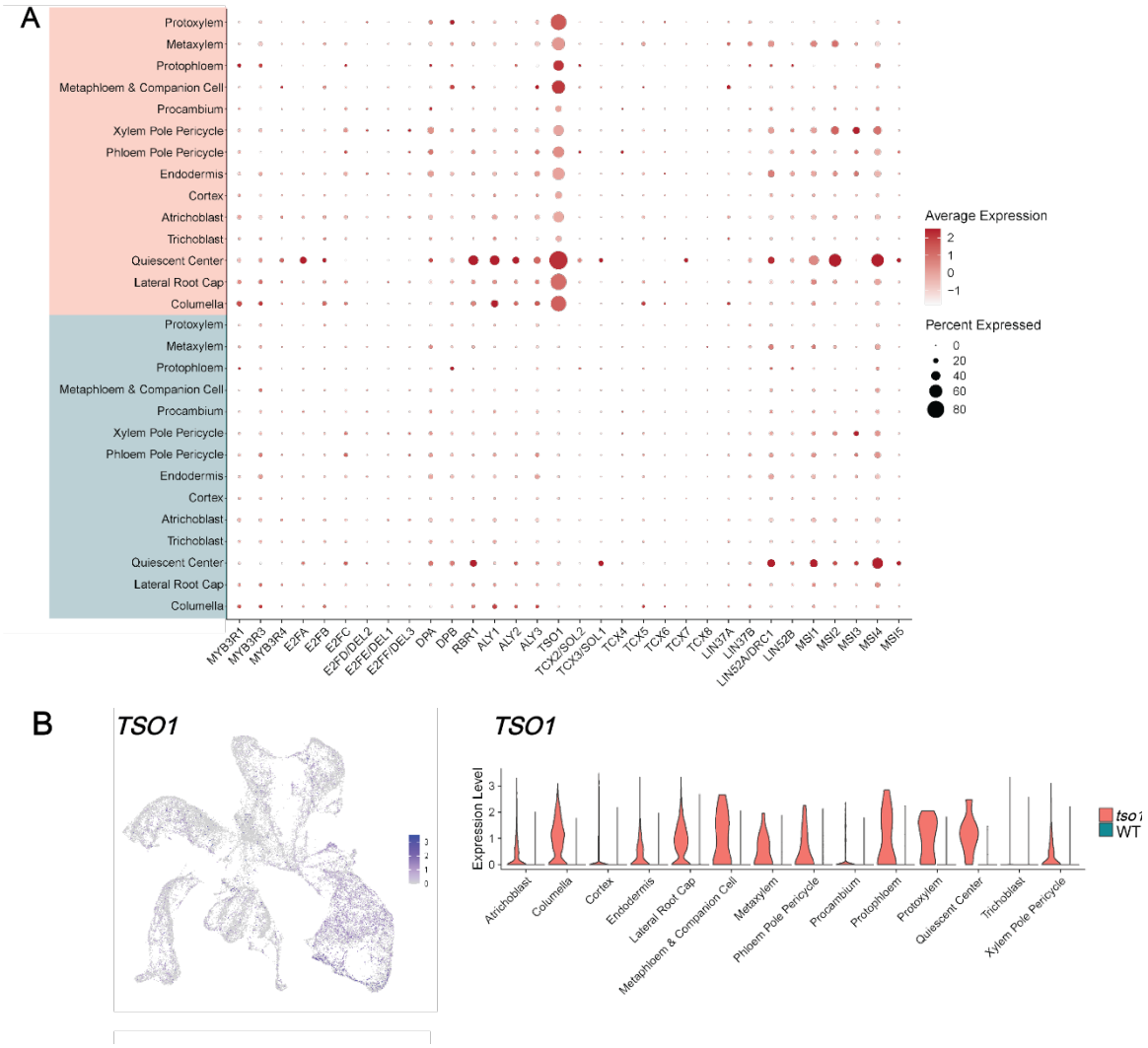

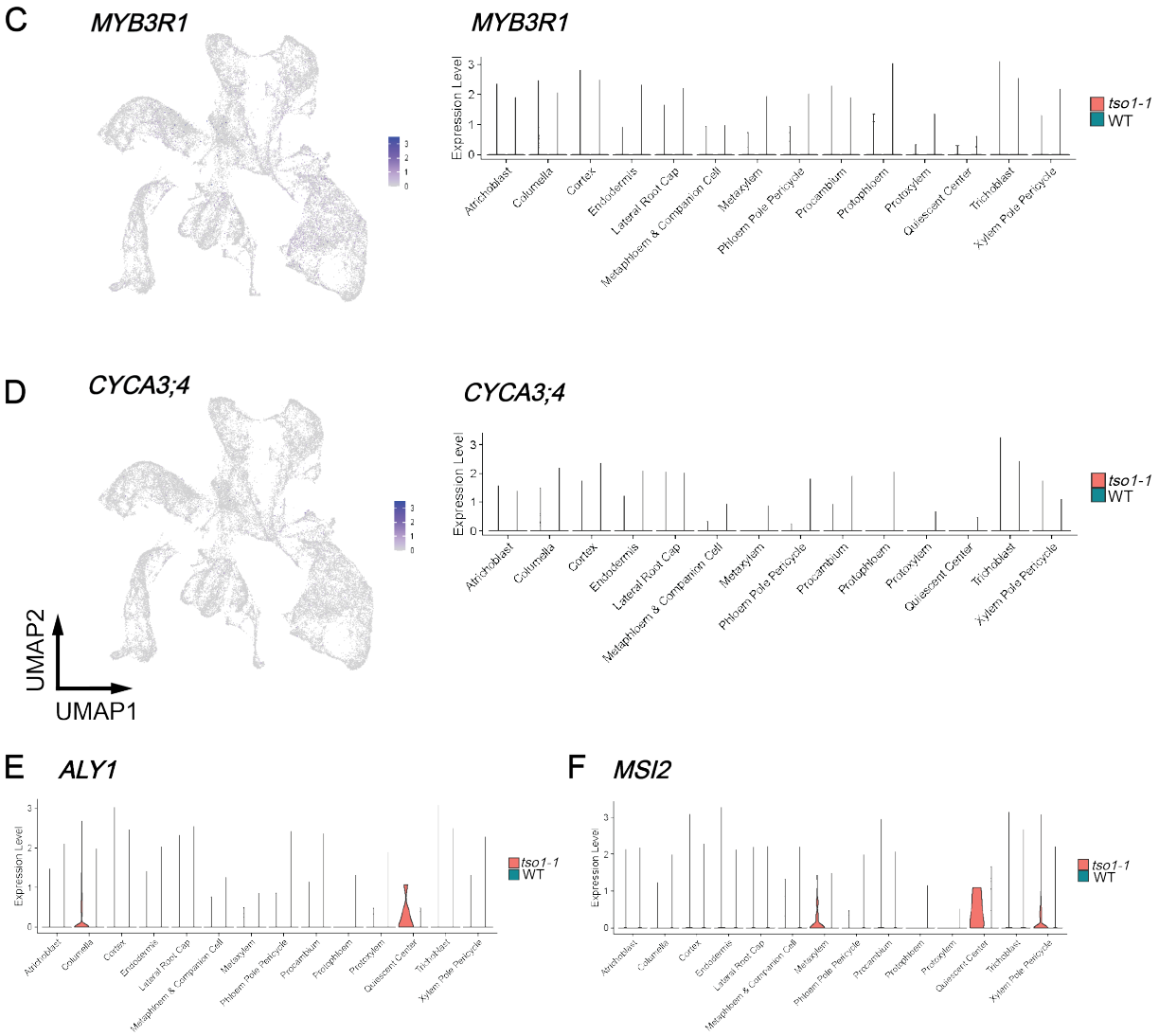

Figure 3.3: *TSO1* is both ectopic and overexpressed in *tso1-1* root cells.
(A) A dot plot showing the expression patterns of the plant DREAM components. X-axis shows potential plant DREAM complex component. Y-axis shows different cell types in WT (grey shade) *and tso1-1* (pink shade) samples. The size of a dot represents the percentage of the cells in a tissue expressing the of interest. The color of a dot represents the average expression level of a particular gene in log transformed expression scaled by Seurat. (B)-(D) Feature plots (left panel) showing the cells expressing *TSO1* (B), *MYB3R1* (C), and *CYCA3;4* (D) and violin plots (right panel) showing the tissue-specific expression in log transformed expression normalized by Seurat. There are fewer cells expressing *MYB3R1* or *CYCA3;4* than those expressing *TSO1*. No significant changes in expression of *MYB3R1* and *CYCA3*;4 are detected in the violin plot. (E)-(F) are violin plots of ALY1 and MSI2.

complex components (*TSO1, MYB3R1, ALY1* and *MSI2*) in specific cell types, in particular, QC to maintain stem cell identity.

3.2.3 Both cell type and cell numbers that express *HD-ZIP III*s are altered in *tso1-1* root cells

HD-ZIP III genes are involved in regulating vasculature development (Carlsbecker *et al.*, 2010). The reduction of the percentage of vascular cells (Figure 3.2D) led us to examinate the expression of *HD-ZIP III* genes. In *tso1-1*, the expression of several *HD-ZIP III* members was increased in the vascular tissues (Figure 3.4 A). The violin plot shows more cells in the *tso1-1* metaxylem express *PHB* than wild type, while the average expression level of *PHB* per cell changes only slightly in *tso1-1* (Figure 3.4 A and B). The *REV and ATHB8* show ectopic expression in some of the *tso1-1* vascular cells. Cells in procambium and protophloem express *REV* in *tso1-1,* but hardly any corresponding cells in WT express *REV;* some cells in *tso1-1* protoxylem express *ATHB8,* but almost none in WT protoxylem express *ATHB8* (Figure 3.4B). On the other hand, while significantly more *tso1-1* QC cells express REV, significantly fewer QC cells in WT express *ATHB8*. Overall, *HD-ZIP III* gene expression appears increased or ectopically expressed in the absence of WT *TSO1*, indicating a negative regulatory relationship between *TSO1* and *HD-ZIPIII*.

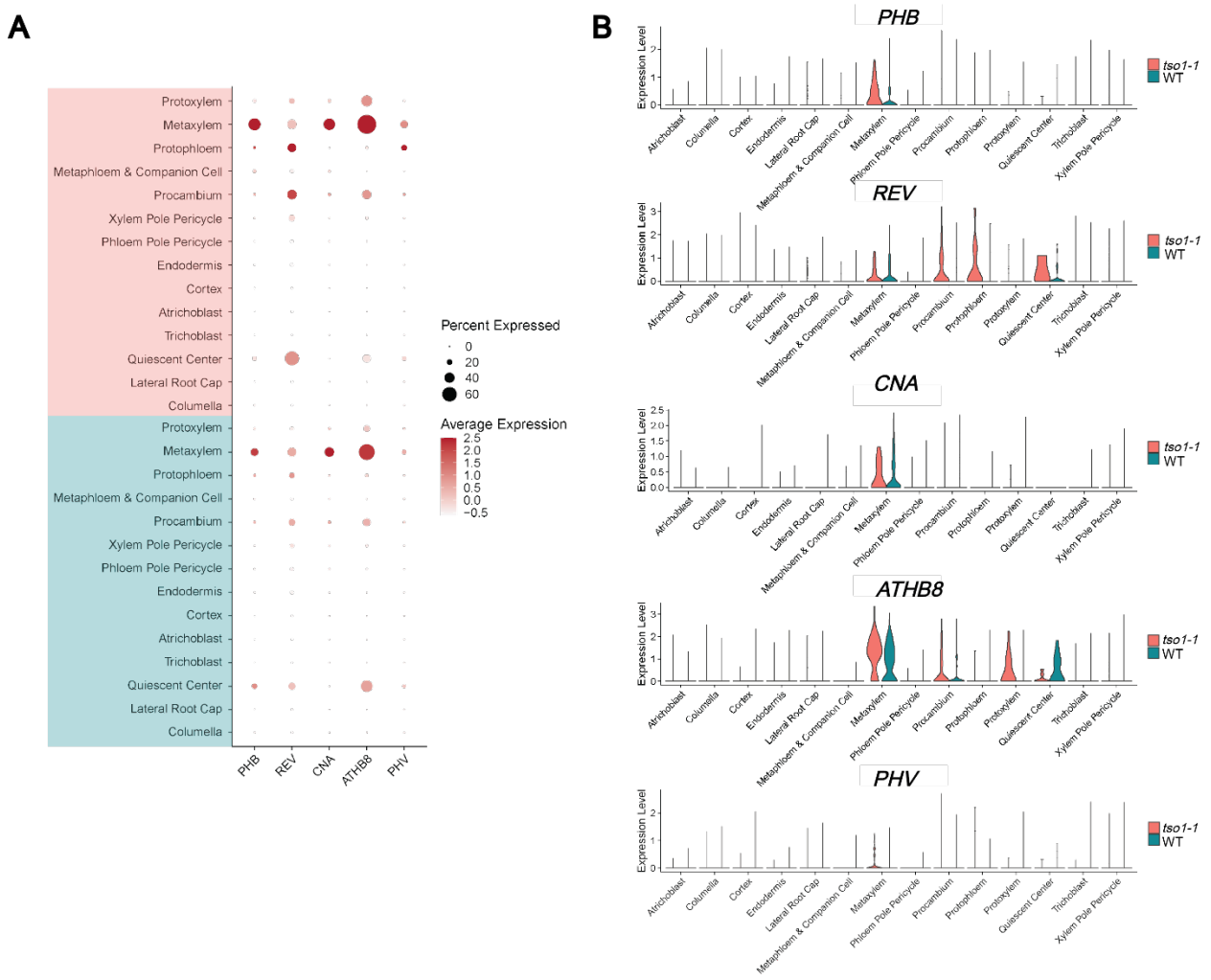

Figure 3.4: The *HD-ZIP III* family of genes are overexpressed or ectopically expressed in *tso1-1* root vasculature tissues.
(A) A dot plot comparing the expression patterns of the *HD-ZIP III* genes in WT (green shade) and *tso1-1* (pink shade). More vascular cells, in particular, metaxylem and procambium, are overexpressing the *HD-ZIP III*s in *tso1-1* root. (B) Violin plots showing the tissue-specific expression patterns of the *HD-ZIP III* genes. *REV* and *ATHB8* are ectopically expressed in some of the vascular tissues, while more metaxylem cells express *PHB*. Y-axis shows log transformed expression normalized by Seurat.

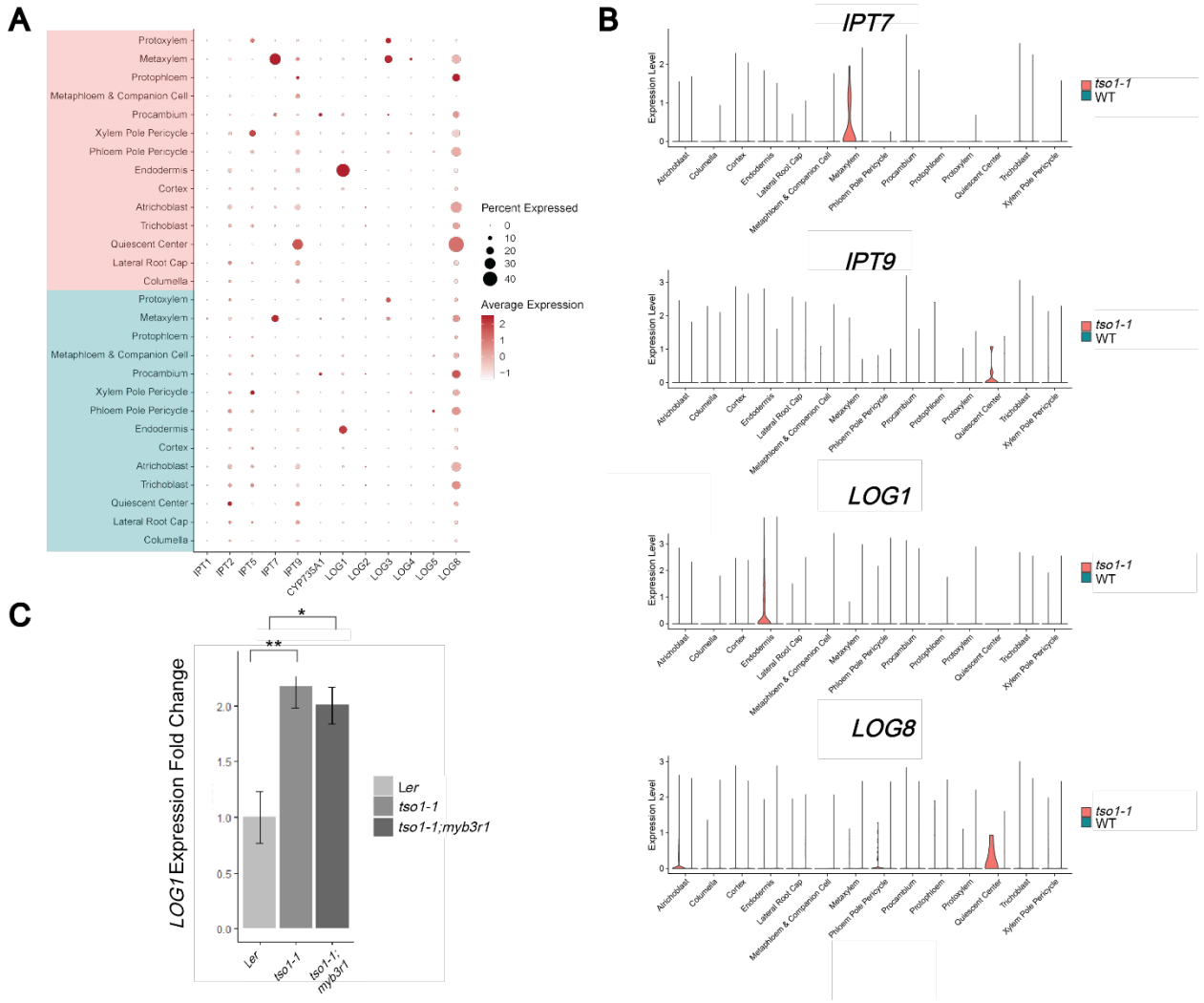

Figure 3.5: The expression of cytokinin biosynthesis genes is increased in specific *tso1-1* root cells.
(A) A dotplot showing the comparison of cytokinin biosynthesis gene expression in wild type (green) and *tso1-1* (pink) root. The expression of *IPT7, IPT9, LOG1* and *LOG8* are altered in *tso1-1*. (B) Violin plots showing tissue-specific expression of *IPT7*, *IPT9*, *LOG1* and *LOG8*. A significant higher number of metaxylem cells express *IPT7* in *tso1-1,* while a higher number of endodermal cells express *LOG1* in *tso1-1*. A larger number of QC cells express *IPT9* and *LOG8* in *tso1-1* when compared with WT. (C) RT-qPCR showing that *LOG1* is overexpressed in *tso1-1* shoot apical meristem. ** stands for $p < 0.05$, * stands for $p < 0.1$ (One-way ANOVA and Tukey's test).

3.2.4 Expression of cytokinin biosynthesis genes is increased in *tso1-1* root

The finding of increased *HD-ZIP III* gene expression in *tso1-1* is exciting, as *PHB* regulates cytokinin biosynthesis in the vascular tissues (Dello Ioio *et al.*, 2012). It activates the expression of a gene named *ISOPENTENYLTRANSFERASE 7* (*IPT7*), which encodes a rate-limiting enzyme for cytokinin biosynthesis. The previously characterized *tso1-1* short root phenotype resembles the short root phenotype caused by exogenous application of cytokinin (Dello Ioio *et al.*, 2007; Wang *et al.*, 2018). The RAM size of *Arabidopsis* root was reduced when treated with cytokinin, probably due to the early cellular differentiation of RAM cells facilitated by increased cytokinin (Dello Ioio *et al.*, 2007). This phenotype is also observed in the *tso1-1* root (reduced RAM size and premature cell differentiation). Therefore, we hypothesize that the short root phenotype of *tso1-1* could be mediated by elevated cytokinin.

In our scRNA-seq data, several cytokinin biosynthesis genes, in particular *IPT7*, *IPT9*, *LOG1*, and *LOG8*, are found ectopically expressed in specific root tissues (Figure3.5 A). In the violin plots, both the number of metaxylem cells that express *IPT7* and the expression level of IPT7 are increased in *tso1-1* relative to WT root (Figure3.5 B). This is consistent with a similar expression change of *PHB* in the *tso1-1* metaxylem (Figure3.4 B), in support of *PHB*'s role in the activation of *IPT7* in metaxylem. The *IPT9* is increased in the QC, suggesting tissue-specific regulation of *IPT* genes (Figure 3.5 B). Another family of cytokinin biosynthetic enzyme is called the *LONELY GUY* (*LOG*) family. The expression of two members of the *LOG* family is elevated in the *tso1-1* root: *LOG1* is specifically overexpressed in the endodermis while *LOG8* is overexpressed in both atrichoblast and QC. These observations

support our hypothesis that loss of *TSO1* may result in increased cytokinin and earlier differentiation, leading to the short root phenotype.

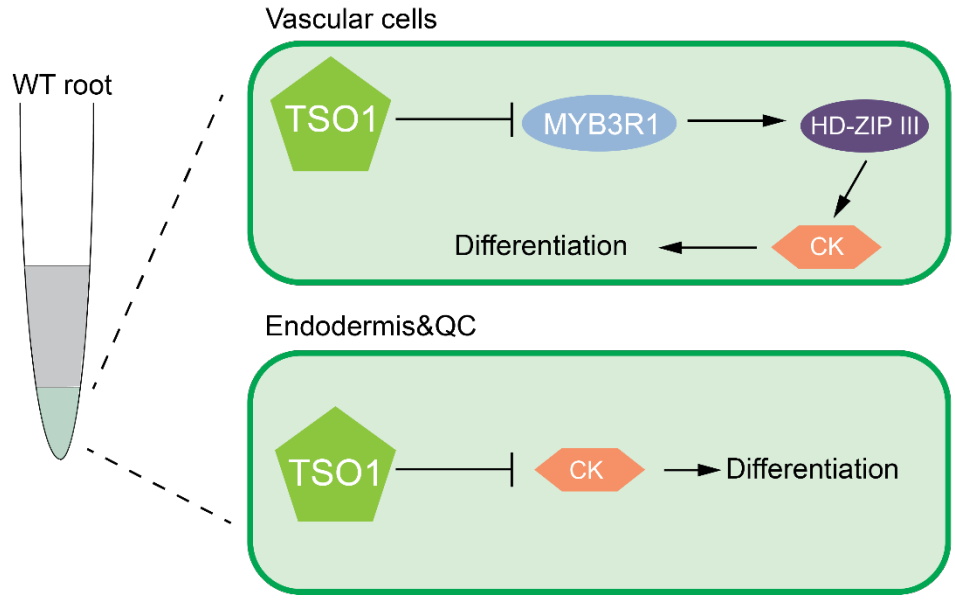

Figure 3.6: A regulatory pathway consisting of *TSO1*, *MYB3R1*, *HD-ZIP III* and cytokinin (CK) that controls cell differentiation in *Arabidopsis* root.
Based on the comparison of single cell RNA profiles of wild type and *tso1-1*, two tissue-specific regulatory modules of *TSO1* are proposed. In wild type vascular cells, the HD-ZIP III proteins activate cytokinin synthesis to induce cell differentiation in the root. *TSO1* represses the expression of the *HD-ZIP III* genes by inhibiting the expression of *MYB3R1*. Ectopic overexpression of HD-ZIPIII in *tso1-1* mutant roots causes increased cytokinin biosynthesis that leads to precocious differentiation. In endodermis and QC, *TSO1* represses cytokinin synthesis to help maintain stem cell identity. Arrows and bars do not imply direct regulation.

3.3 Discussion

3.3.1 TSO1 represses *HD-ZIP III* genes to inhibit cytokinin synthesis, which prevents premature root cell differentiation

Previous studies have revealed that *TSO1* plays important roles in regulating SAM and RAM size. The *tso1-1* mutant has enlarged and fasciated shoot apical meristem due to over-proliferation (Liu, Running and Meyerowitz, 1997). Meanwhile, the *tso1-1* mutant also produces much shorter root compared to wild type (Wang *et al.*, 2018).

The short root phenotype was caused by premature cell cycle exit and precocious cellular differentiation at RAM. The underlying molecular mechanism of *TSO1* function in RAM is still lacking, especially how a loss of *TSO1* leads to premature cell cycle exit.

The root length is regulated in part by how soon the cells begin to differentiate at the transition zone, where cells exit cell cycle permanently and start to elongate (Baluska, Volkmann and Barlow, 1996). The transition zone is an active site for hormone crosstalk (Kong *et al.*, 2018). Cytokinin controls RAM size by positioning the transition zone (Dello Ioio *et al.*, 2007). Specifically, it acts in the vascular tissues in the transition zone to activate a repressor of auxin signaling gene *SHORT HYPOCOTYL2 (SHY2)* to promote cell differentiation (Dello Ioio *et al.*, 2008). In addition, exogenous application of cytokinin led to premature cell cycle exit and differentiation (Dello Ioio *et al.*, 2007), causing short root phenotype. This led to the hypothesis that the short root of *tso1-1* might be related to increased cytokinin.

The comparison of the scRNA-seq data of *tso1-1* and wild type roots provided unprecedented details of *TSO1* regulatory networks. One important observation is that the expression *HD-ZIP III* family members in root is increased in the *tso1-1* metaxylem, a subtissue of vasculature. Since the gain-of-function *HD-ZIP III* mutants, *phb-1d* and *phv-1d*, have much shorter roots and significantly smaller RAMs than the wild type (Dello Ioio *et al.*, 2012), the observed over-expression of *PHB* and *PHV* in the *tso1-1* metaxylem may mediate the *tso1-1* short root phenotype. Moreover, *PHB* and *PHV* have been demonstrated as positive regulators of a cytokinin biosynthesis gene *IPT7*. Among them, *PHB* is necessary and sufficient to

directly activate the expression of *IPT7* in the vascular tissues, leading to the production of cytokinin (Dello Ioio *et al.*, 2012). Therefore, increased *IPT7* expression in the *tso1-1* metaxylem, as revealed my our scRNA-seq data, suggests that *TSO1* regulates root development by regulating cytokinin biosynthesis in specific root cells and this regulation is likely achieved indirectly by repressing *PHB* and *PHV* expression (Figure 3.6).

3.3.2 Integration of *MYB3R1* in the *TSO1* network

Previous studies showed that the *tso1-1* short root phenotype could be attributed to the overexpression of *MYB3R1* as removing *MYB3R1* by a loss-of-function mutation suppressed the short root phenotype. However, it was unclear why an overexpression of *MYB3R1* induces early root cell differentiation and short root phenotype. Is *MYB3R1* function related to the *HD-ZIP III* genes or do *MYB3R1* and *HD-ZIPIII* act in parallel pathways? Recent studies revealed the potential genetic relationship between *MYB3R1* and the *HD-ZIP III*s. A chromatin immunoprecipitation sequencing (ChIP-seq) that aims at identifying MYB3R1 binding sites revealed *PHB*, *REV* and *ATHB8* as the potential regulatory targets of MYB3R1 (Yang *et al.*, 2021). While the experiment was performed using shoot meristem cells, the regulatory relationship could be preserved in the root cells. Therefore, *TSO1* may repress the expression of the *HD-ZIP III* genes through the inhibition of *MY3BR1* expression (Figure3.6).

3.3.3 The increased expression of the *HD-ZIP III* genes affects vasculature development

In addition to controlling cytokinin biosynthesis, the *HD-ZIP III* genes are also known as regulators of vascular patterning in *Arabidopsis* (Zhou *et al.*, 2007;

Carlsbecker *et al.*, 2010). Losing all five members of the *HD-ZIP III* family leads to failure of xylem formation, however, the quadruple mutant *athb8-11 cna-2 phb-13 phv-11* generates more vascular cells (Carlsbecker *et al.*, 2010). It seems that the *HD-ZIP III* genes are necessary for xylem formation but restrict vascular cell proliferation at the same time. Therefore, upregulation of the *HD-ZIP III* genes may result in fewer vascular cells. The discovery of increased expression of multiple *HD-ZIP III* genes and reduction of the vascular cells in *tso1-1* (Figure 3.2) support this hypothesis. It suggests that *TSO1* regulate vasculature development through regulating *HD-ZIP III*s. It will be interesting to examine the vascular tissues of *tso1-1* in the root as well as shoot to see if there's any existing developmental defects.

3.3.4 Overexpression of *LOG1* suggest *TSO1* may regulate cytokinin synthesis in SAM

Besides the increased expression of *IPT7 in* the vasculature, increased expression of cytokinin biosynthesis genes was also detected in other tissues. The upregulation of *LOG1*, *IPT9* and *LOG8* suggests that *TSO1* regulates cytokinin biosynthesis not only in the vascular tissues but also in the endodermis and QC through unknown mechanisms. Though no significant morphological change of these tissues was observed under the microscope, nor from the scRNA-seq data, the gene expression network might be altered in these tissues in *tso1-1* mutant (Wang *et al.*, 2018). Compared to the wild type, the expression of *LOG1* increased about one-fold in *tso1-1* shoot (Figure 3.5C), indicating there might be over-production of cytokinin in the SAM. Therefore, there are potentially conserved regulatory relationships between *TSO1* and cytokinin synthesis in root as well as shoot. In fact, the enlargement of the *tso1-1* SAM resembles the phenotype of applying cytokinin to the *Arabidopsis* SAM

(Giulini, Wang and Jackson, 2004). It is possible that the enlargement of *tso1-1* SAM can be attributed, at least partially, to the increased cytokinin at the shoot.

3.3.5 *TSO1* is involved in regulation of itself and plant DREAM complex components

The scRNA transcriptomes of wild type and *tso1-1* roots show that *TSO1* is highly and ectopically expressed in nearly all cell types in the *tso1-1* roots. Therefore, *TSO1* may repress the expression of itself in most root cell types. Besides *TSO1*, two other plant DREAM complex component, *ALY1* and *MSI2*, are found overexpressed in *tso1-1*, suggesting that *TSO1* regulates the spatial expression of potential plant DREAM complex components in root to balance cell division and cell differentiation in the RAM. In addition, it was reported that the *tso1-1* mutant protein can interfere with the function of its close homolog *SOL2* and knocking down of the *tso1-1* transcript partially rescue the fasciation phenotype, suggesting the tso1-1 protein might be poisonous for plant meristem development (Sijacic, Wang and Liu, 2011). It is possible that the over-accumulated *tso1-1* disrupt the function of its homolog, resulting in defects of root cell development.

3.4 Methods

3.4.1 Protoplast isolation and scRNA-seq

1,000-3,500 primary roots per sample were cut from the tip (~0.5cm, 5DPG) and used for protoplasting. Protoplast isolation followed a protocol described in a previous publication (Shahan *et al.*, 2022). The protoplast suspension was then loaded onto microfluidic chips (10X Genomics) to capture 5,000 or 10,000 cells per sample. Barcoding of cells was carried out with a Chromium Controller (10X Genomics). The

mRNA isolation, reverse transcription and Illumina library preparation also followed the protocol in the same publication (Shahan *et al.*, 2022). The samples were sequenced with a Novaseq 6000 (Illumina) to generate 100bp pair-end reads.

3.4.2 scRNA-seq data pre-processing

Cell Ranger (v4.0.0) was applied to generate the row count matrices from FASTQ files for each sample (Zheng *et al.*, 2017). Original STAR within the Cell Ranger was replaced by STAR (v2.7.3a) because of system incompatibility. TAIR10_chr_all.fas (https://www.arabidopsis.org/download_files/Genes/TAIR10_genome_release/TAIR10_chromosome_files/TAIR10_chr_all.fas) and Araport11_GFF3_genes_transposons.201606.gtf.gz (https://arabidopsis.org/download_files/Genes/Araport11_genome_release/archived/Araport11_GFF3_genes_transposons.201606.gff.gz) were used as the *Arabidopsis* reference genome and annotation, respectively.

3.4.3 Label transfer and integration

Seurat (v3.2.3) was utilized to transfer the annotations from the published atlas to the WT and *tso1-1* mutant samples (Satija *et al.*, 2015; Shahan *et al.*, 2022). The cells that had greater than 5% mitochondrial and chloroplast counts were filtered out. And the genes affected by protoplasting (https://github.com/Hsu-Che-Wei/COPILOT/blob/master/supp_data/Protoplasting_DEgene_FC2_list.txt) were removed from the analyses. Additionally, data normalization was performed using SCTransform approach. The WT and mutant Seurat objects were further integrated, and the RNA assay was normalized and scaled for downstream visualization after integration.

3.4.4 RNA extraction and RT-qPCR experiments

Arabidopsis SAMs were collected for RNA extraction using RNeasy Mini Kit (Qiagen). RNA samples were cleaned with DNase I. cDNAs were synthesized using RevertAid First Strand cDNA Synthesis Kit (ThermoFisher). RT-qPCR experiments were performed on the Bio-rad CFX 96 machine with PowerUp™ SYBR® Green Master Mix (Thermo Fisher). Three biological replicates were conducted for the RT-qPCR with three technical replicates. The *TIP41(AT4G34270)* gene was used as the internal control.

Chapter 4: Conclusion and future direction

4.1 Conclusion

In summary, I characterized a genetic suppressor of the *tso1-1* mutant. It suppresses the SAM fasciation and partially restores the sterility of the *tso1-1* mutant. The causal mutation was mapped to a G-to-A mutation in a A-type cyclin gene, *CYCA3;4*. I showed that the expression of *CYCA3;4* was increased in the *tso1-1* SAM, suggesting that the overexpression of *CYCA3;4* mediates the *tso1-1* shoot phenotype. I also found that *TSO1* might regulate the expression of *CYCA3;4* indirectly by repressing *MYB3R1* transcription in wild type plants.

In collaboration with two other scientists, I analyzed the *tso1-1* root phenotype by applying single cell RNA sequencing. I found that the short root phenotype of *tso1-1* might be caused by defects in the vasculature development but not by the absence of certain cell types. By looking at the gene expression profiles, I discovered that the *HD-ZIP III* genes and several cytokinin biosynthesis genes are ectopically expressed in *tso1-1* root, which indicates that the *tso1-1* short root phenotype might be attributed to over-production of cytokinin.

4.2 Future directions

Why the mutations in *CYCA3;4* only partially suppressed the shoot phenotype and did not suppress the root phenotype? It leads to the questions that whether there is redundancy among the *CYCA3* genes. It is unclear whether TSO1 can regulate the expression of other *CYCA3*s and whether the regulation is achieved in a similar manner.

Generating double knock-out or triple knock-out of *CYCA3*s in the *tso1-1* background and observing if there are better suppression effects than the single knock-out of *CYCA3;4* can help us answer the redundancy question. It can also help understand the roles of these cyclins in the *TSO1* regulatory pathway and how *TSO1* participates in the cell cycle regulation at molecular level.

In addition, the result from the scRNA-seq suggests that TSO1 may regulate the expression of the *HD-ZIPIII* genes and several cytokinin biosynthesis genes in the root. One simple question is that whether the regulation pathways are similar or even the same in the shoot? To answer this question, we have examined the shoot phenotype of the *tso1-1; rev* double mutant plants and found that knock-out of the *REV* gene suppressed the fasciation of the *tso1-1* SAM. Therefore, we proposed that TSO1 might regulate the *HD-ZIPIII* genes in both *Arabidopsis* shoot and root.

It will be interesting to test this hypothesis by looking at the phenotype of other TSO1 and *HD-ZIPIII*s double knockout mutants.

One of the experiments could be done to validate our scRNA-seq results, transcriptional reporters like promoter fusing to GFP can be used to examine the expression of the *HD-ZIP III* genes as well as *IPT7*, *IPT9*, *LOG1* and *LOG8* in *tso1-1* root. It can help to determine if the expression domains of these genes expand, or the expression levels are increased compared to the wild type.

The finding of increased cytokinin biosynthesis is also quite interesting. It provides insights of how conserved cell cycle machineries can regulate plant development through regulating the plant hormones. Similar to the proposed experiments for the *HD-ZIPIII* genes, generating the knockouts of the cytokinin genes found in the

scRNA-seq analysis and observing if they suppress the short root phenotype of *tso1-1* can further confirm the proposed *TSO1* regulatory pathway. Besides the cytokinin biosynthesis synthesis, we are curious about the cytokinin response in *tso1-1* root too. Existing synthetic cytokinin reporters (Liu and Müller, 2017) can be used to compare the response in the *tso1-1* and the wild type roots.

Bibliography

Aida, M. *et al.* (2004) 'The PLETHORA Genes Mediate Patterning of the Arabidopsis Root Stem Cell Niche', *Cell*, 119(1), pp. 109–120. Available at: https://doi.org/10.1016/j.cell.2004.09.018.

Andersen, S.U. *et al.* (2007) 'The conserved cysteine-rich domain of a tesmin/TSO1-like protein binds zinc in vitro and TSO1 is required for both male and female fertility in Arabidopsis thaliana', *Journal of Experimental Botany*, 58(13), pp. 3657–3670. Available at: https://doi.org/10.1093/jxb/erm215.

Araki, S. *et al.* (2004) 'Mitotic Cyclins Stimulate the Activity of c-Myb-like Factors for Transactivation of G2/M Phase-specific Genes in Tobacco *', *Journal of Biological Chemistry*, 279(31), pp. 32979–32988. Available at: https://doi.org/10.1074/jbc.M403171200.

Baluska, F., Volkmann, D. and Barlow, P.W. (1996) 'Specialized Zones of Development in Roots: View from the Cellular Level', *Plant Physiology*, 112(1), pp. 3–4. Available at: https://doi.org/10.1104/pp.112.1.3.

Beall, E.L. *et al.* (2007) 'Discovery of tMAC: a Drosophila testis-specific meiotic arrest complex paralogous to Myb–Muv B', *Genes & Development*, 21(8), pp. 904–919. Available at: https://doi.org/10.1101/gad.1516607.

Benfey, P.N. *et al.* (1993) 'Root development in Arabidopsis: four mutants with dramatically altered root morphogenesis', *Development*, 119(1), pp. 57–70. Available at: https://doi.org/10.1242/dev.119.1.57.

Blilou, I. *et al.* (2005) 'The PIN auxin efflux facilitator network controls growth and patterning in Arabidopsis roots', *Nature*, 433(7021), pp. 39–44. Available at: https://doi.org/10.1038/nature03184.

Boruc, J. *et al.* (2010) 'Functional Modules in the Arabidopsis Core Cell Cycle Binary Protein–Protein Interaction Network', *The Plant Cell*, 22(4), pp. 1264–1280. Available at: https://doi.org/10.1105/tpc.109.073635.

Bulankova, P. *et al.* (2013) 'Identification of Arabidopsis Meiotic Cyclins Reveals Functional Diversification among Plant Cyclin Genes', *PLOS Genetics*, 9(5), p. e1003508. Available at: https://doi.org/10.1371/journal.pgen.1003508.

Carlsbecker, A. *et al.* (2010) 'Cell signalling by microRNA165/6 directs gene dose-dependent root cell fate', *Nature*, 465(7296), pp. 316–321. Available at: https://doi.org/10.1038/nature08977.

Chickarmane, V.S. *et al.* (2012) 'Cytokinin signaling as a positional cue for patterning the apical–basal axis of the growing Arabidopsis shoot meristem', *Proceedings of the National Academy of Sciences*, 109(10), pp. 4002–4007. Available at: https://doi.org/10.1073/pnas.1200636109.

Clark, S.E., Running, M.P. and Meyerowitz, E.M. (1995) 'CLAVATA3 is a specific regulator of shoot and floral meristem development affecting the same processes as CLAVATA1', *Development*, 121(7), pp. 2057–2067. Available at: https://doi.org/10.1242/dev.121.7.2057.

Clark, S.E., Williams, R.W. and Meyerowitz, E.M. (1997) 'The CLAVATA1Gene Encodes a Putative Receptor Kinase That Controls Shoot and Floral Meristem Size in Arabidopsis', *Cell*, 89(4), pp. 575–585. Available at: https://doi.org/10.1016/S0092-8674(00)80239-1.

Cui, H. *et al.* (2007) 'An Evolutionarily Conserved Mechanism Delimiting SHR Movement Defines a Single Layer of Endodermis in Plants', *Science*, 316(5823), pp. 421–425. Available at: https://doi.org/10.1126/science.1139531.

Curtis, M.D. and Grossniklaus, U. (2003) 'A gateway cloning vector set for high-throughput functional analysis of genes in planta', *Plant Physiology*, 133(2), pp. 462–469. Available at: https://doi.org/10.1104/pp.103.027979.

Daum, G. *et al.* (2014) 'A mechanistic framework for noncell autonomous stem cell induction in Arabidopsis', *Proceedings of the National Academy of Sciences*, 111(40), pp. 14619–14624. Available at: https://doi.org/10.1073/pnas.1406446111.

David-Pfeuty, T. and Nouvian-Dooghe, Y. (1996) 'Human cyclin B1 is targeted to the nucleus in G1 phase prior to its accumulation in the cytoplasm', *Oncogene*, 13(7), pp. 1447–1460.

De Rybel, B. *et al.* (2016) 'Plant vascular development: from early specification to differentiation', *Nature Reviews Molecular Cell Biology*, 17(1), pp. 30–40. Available at: https://doi.org/10.1038/nrm.2015.6.

Dello Ioio, R. *et al.* (2007) 'Cytokinins Determine Arabidopsis Root-Meristem Size by Controlling Cell Differentiation', *Current Biology*, 17(8), pp. 678–682. Available at: https://doi.org/10.1016/j.cub.2007.02.047.

Dello Ioio, R. *et al.* (2008) 'A Genetic Framework for the Control of Cell Division and Differentiation in the Root Meristem', *Science*, 322(5906), pp. 1380–1384. Available at: https://doi.org/10.1126/science.1164147.

Dello Ioio, R. *et al.* (2012) 'A PHABULOSA/Cytokinin Feedback Loop Controls Root Growth in Arabidopsis', *Current Biology*, 22(18), pp. 1699–1704. Available at: https://doi.org/10.1016/j.cub.2012.07.005.

Denyer, T. *et al.* (2019) 'Spatiotemporal Developmental Trajectories in the Arabidopsis Root Revealed Using High-Throughput Single-Cell RNA Sequencing', *Developmental Cell*, 48(6), pp. 840-852.e5. Available at: https://doi.org/10.1016/j.devcel.2019.02.022.

Earley, K.W. *et al.* (2006) 'Gateway-compatible vectors for plant functional genomics and proteomics', *The Plant Journal*, 45(4), pp. 616–629. Available at: https://doi.org/10.1111/j.1365-313X.2005.02617.x.

Emery, J.F. *et al.* (2003) 'Radial Patterning of Arabidopsis Shoots by Class III HD-ZIP and KANADI Genes', *Current Biology*, 13(20), pp. 1768–1774. Available at: https://doi.org/10.1016/j.cub.2003.09.035.

Fischer, M. and Müller, G.A. (2017) 'Cell cycle transcription control: DREAM/MuvB and RB-E2F complexes', *Critical Reviews in Biochemistry and Molecular Biology*, 52(6), pp. 638–662. Available at: https://doi.org/10.1080/10409238.2017.1360836.

Fletcher, J.C. *et al.* (1999) 'Signaling of Cell Fate Decisions by CLAVATA3 in Arabidopsis Shoot Meristems', *Science* [Preprint]. Available at: https://doi.org/10.1126/science.283.5409.1911.

Forzani, C. *et al.* (2014) 'WOX5 Suppresses CYCLIN D Activity to Establish Quiescence at the Center of the Root Stem Cell Niche', *Current Biology*, 24(16), pp. 1939–1944. Available at: https://doi.org/10.1016/j.cub.2014.07.019.

Galinha, C. *et al.* (2007) 'PLETHORA proteins as dose-dependent master regulators of Arabidopsis root development', *Nature*, 449(7165), pp. 1053–1057. Available at: https://doi.org/10.1038/nature06206.

Gälweiler, L. *et al.* (1998) 'Regulation of Polar Auxin Transport by AtPIN1 in Arabidopsis Vascular Tissue', *Science*, 282(5397), pp. 2226–2230. Available at: https://doi.org/10.1126/science.282.5397.2226.

Gibson, D.G. *et al.* (2009) 'Enzymatic assembly of DNA molecules up to several hundred kilobases', *Nature Methods*, 6(5), pp. 343–345. Available at: https://doi.org/10.1038/nmeth.1318.

Giulini, A., Wang, J. and Jackson, D. (2004) 'Control of phyllotaxy by the cytokinin-inducible response regulator homologue ABPHYL1', *Nature*, 430(7003), pp. 1031–1034. Available at: https://doi.org/10.1038/nature02778.

Gordon, S.P. *et al.* (2009) 'Multiple feedback loops through cytokinin signaling control stem cell number within the Arabidopsis shoot meristem', *Proceedings of the National Academy of Sciences*, 106(38), pp. 16529–16534. Available at: https://doi.org/10.1073/pnas.0908122106.

Grieneisen, V.A. *et al.* (2007) 'Auxin transport is sufficient to generate a maximum and gradient guiding root growth', *Nature*, 449(7165), pp. 1008–1013. Available at: https://doi.org/10.1038/nature06215.

Haga, N. *et al.* (2007) 'R1R2R3-Myb proteins positively regulate cytokinesis through activation of KNOLLE transcription in Arabidopsis thaliana', *Development*, 134(6), pp. 1101–1110. Available at: https://doi.org/10.1242/dev.02801.

Haga, N. *et al.* (2011) 'Mutations in MYB3R1 and MYB3R4 Cause Pleiotropic Developmental Defects and Preferential Down-Regulation of Multiple G2/M-Specific Genes in Arabidopsis1[C][W]', *Plant Physiology*, 157(2), pp. 706–717. Available at: https://doi.org/10.1104/pp.111.180836.

Harashima, H. and Schnittger, A. (2012) 'Robust reconstitution of active cell-cycle control complexes from co-expressed proteins in bacteria', *Plant Methods*, 8(1), p. 23. Available at: https://doi.org/10.1186/1746-4811-8-23.

Harrison, M.M. *et al.* (2006) 'Some C. elegans class B synthetic multivulva proteins encode a conserved LIN-35 Rb-containing complex distinct from a NuRD-like complex', *Proceedings of the National Academy of Sciences*, 103(45), pp. 16782–16787. Available at: https://doi.org/10.1073/pnas.0608461103.

Hauser, B.A. *et al.* (2000) 'TSO1 is a novel protein that modulates cytokinesis and cell expansion in Arabidopsis', *Development*, 127(10), pp. 2219–2226. Available at: https://doi.org/10.1242/dev.127.10.2219.

Hauser, B.A., Villanueva, J.M. and Gasser, C.S. (1998) 'Arabidopsis TSO1 Regulates Directional Processes in Cells During Floral Organogenesis', *Genetics*, 150(1), pp. 411–423.

Helariutta, Y. *et al.* (2000) 'The SHORT-ROOT Gene Controls Radial Patterning of the Arabidopsis Root through Radial Signaling', *Cell*, 101(5), pp. 555–567. Available at: https://doi.org/10.1016/S0092-8674(00)80865-X.

Higuchi, M. *et al.* (2004) 'In planta functions of the Arabidopsis cytokinin receptor family', *Proceedings of the National Academy of Sciences*, 101(23), pp. 8821–8826. Available at: https://doi.org/10.1073/pnas.0402887101.

Hollender, C.A. *et al.* (2012) 'Flower and early fruit development in a diploid strawberry, Fragaria vesca', *Planta*, 235(6), pp. 1123–1139. Available at: https://doi.org/10.1007/s00425-011-1562-1.

Iness, A.N. *et al.* (2019) 'The cell cycle regulatory DREAM complex is disrupted by high expression of oncogenic B-Myb', *Oncogene*, 38(7), pp. 1080–1092. Available at: https://doi.org/10.1038/s41388-018-0490-y.

Jeong, S., Trotochaud, A.E. and Clark, S.E. (1999) 'The Arabidopsis CLAVATA2 Gene Encodes a Receptor-like Protein Required for the Stability of the CLAVATA1 Receptor-like Kinase', *The Plant Cell*, 11(10), pp. 1925–1933. Available at: https://doi.org/10.1105/tpc.11.10.1925.

Kieber, J.J. (2002) ‘Cytokinins’, *The Arabidopsis Book*, 2002(1). Available at: https://doi.org/10.1199/tab.0063.

Kim, J. *et al.* (2005) ‘microRNA-directed cleavage of ATHB15 mRNA regulates vascular development in Arabidopsis inflorescence stems’, *The Plant journal : for cell and molecular biology*, 42(1), pp. 84–94. Available at: https://doi.org/10.1111/j.1365-313X.2005.02354.x.

Kobayashi, K. *et al.* (2015) ‘Transcriptional repression by MYB3R proteins regulates plant organ growth’, *The EMBO journal*, 34(15), pp. 1992–2007. Available at: https://doi.org/10.15252/embj.201490899.

Kõivomägi, M. *et al.* (2011) ‘Dynamics of Cdk1 substrate specificity during the cell cycle’, *Molecular Cell*, 42(5), pp. 610–623. Available at: https://doi.org/10.1016/j.molcel.2011.05.016.

Kong, X. *et al.* (2018) ‘The Root Transition Zone: A Hot Spot for Signal Crosstalk’, *Trends in Plant Science*, 23(5), pp. 403–409. Available at: https://doi.org/10.1016/j.tplants.2018.02.004.

Korenjak, M. *et al.* (2004) ‘Native E2F/RBF complexes contain Myb-interacting proteins and repress transcription of developmentally controlled E2F target genes’, *Cell*, 119(2), pp. 181–193. Available at: https://doi.org/10.1016/j.cell.2004.09.034.

Lang, L. *et al.* (2021) ‘The DREAM complex represses growth in response to DNA damage in Arabidopsis’, *Life Science Alliance*, 4(12). Available at: https://doi.org/10.26508/lsa.202101141.

Laurenzio, L.D. *et al.* (1996) ‘The SCARECROW Gene Regulates an Asymmetric Cell Division That Is Essential for Generating the Radial Organization of the Arabidopsis Root’, *Cell*, 86(3), pp. 423–433. Available at: https://doi.org/10.1016/S0092-8674(00)80115-4.

Leibfried, A. *et al.* (2005) ‘WUSCHEL controls meristem function by direct regulation of cytokinin-inducible response regulators’, *Nature*, 438(7071), pp. 1172–1175. Available at: https://doi.org/10.1038/nature04270.

Levesque, M.P. *et al.* (2006) ‘Whole-Genome Analysis of the SHORT-ROOT Developmental Pathway in Arabidopsis’, *PLOS Biology*, 4(5), p. e143. Available at: https://doi.org/10.1371/journal.pbio.0040143.

Lewis, P.W. *et al.* (2004) ‘Identification of a Drosophila Myb-E2F2/RBF transcriptional repressor complex’, *Genes & Development*, 18(23), pp. 2929–2940. Available at: https://doi.org/10.1101/gad.1255204.

Litovchick, L. *et al.* (2007) ‘Evolutionarily Conserved Multisubunit RBL2/p130 and E2F4 Protein Complex Represses Human Cell Cycle-Dependent Genes in

Quiescence', *Molecular Cell*, 26(4), pp. 539–551. Available at: https://doi.org/10.1016/j.molcel.2007.04.015.

Liu, J. and Müller, B. (2017) 'Imaging TCSn::GFP, a Synthetic Cytokinin Reporter, in Arabidopsis thaliana', *Methods in Molecular Biology (Clifton, N.J.)*, 1497, pp. 81–90. Available at: https://doi.org/10.1007/978-1-4939-6469-7_9.

Liu, Y. *et al.* (2012) 'CCS52A2/FZR1, a cell cycle regulator, is an essential factor for shoot apical meristem maintenance in Arabidopsis thaliana', *BMC Plant Biology*, 12, p. 135. Available at: https://doi.org/10.1186/1471-2229-12-135.

Liu, Z. *et al.* (2020) 'Global Dynamic Molecular Profiling of Stomatal Lineage Cell Development by Single-Cell RNA Sequencing', *Molecular Plant*, 13(8), pp. 1178–1193. Available at: https://doi.org/10.1016/j.molp.2020.06.010.

Liu, Z., Running, M.P. and Meyerowitz, E.M. (1997) 'TSO1 functions in cell division during Arabidopsis flower development', *Development (Cambridge, England)*, 124(3), pp. 665–672.

Ljung, K. *et al.* (2005) 'Sites and Regulation of Auxin Biosynthesis in Arabidopsis Roots', *The Plant Cell*, 17(4), pp. 1090–1104. Available at: https://doi.org/10.1105/tpc.104.029272.

Macdonald, H. and Stevens, D. (2019) *Biotechnology and Plant Biology*. Scientific e-Resources.

Marceau, A.H. *et al.* (2016) 'Structural basis for LIN54 recognition of CHR elements in cell cycle-regulated promoters', *Nature Communications*, 7(1), p. 12301. Available at: https://doi.org/10.1038/ncomms12301.

Mayer, K.F.X. *et al.* (1998) 'Role of WUSCHEL in Regulating Stem Cell Fate in the Arabidopsis Shoot Meristem', *Cell*, 95(6), pp. 805–815. Available at: https://doi.org/10.1016/S0092-8674(00)81703-1.

McConnell, J.R. and Barton, M.K. (1998) 'Leaf polarity and meristem formation in Arabidopsis', *Development*, 125(15), pp. 2935–2942. Available at: https://doi.org/10.1242/dev.125.15.2935.

Menges, M. *et al.* (2005) 'Global analysis of the core cell cycle regulators of Arabidopsis identifies novel genes, reveals multiple and highly specific profiles of expression and provides a coherent model for plant cell cycle control', *The Plant Journal*, 41(4), pp. 546–566. Available at: https://doi.org/10.1111/j.1365-313X.2004.02319.x.

Miyawaki, K., Matsumoto-Kitano, M. and Kakimoto, T. (2004) 'Expression of cytokinin biosynthetic isopentenyltransferase genes in Arabidopsis: tissue specificity

and regulation by auxin, cytokinin, and nitrate', *The Plant Journal*, 37(1), pp. 128–138. Available at: https://doi.org/10.1046/j.1365-313X.2003.01945.x.

Müller, G.A. *et al.* (2014) 'The CHR site: definition and genome-wide identification of a cell cycle transcriptional element', *Nucleic Acids Research*, 42(16), pp. 10331–10350. Available at: https://doi.org/10.1093/nar/gku696.

Müller, G.A. *et al.* (2016) 'Timing of transcription during the cell cycle: Protein complexes binding to E2F, E2F/CLE, CDE/CHR, or CHR promoter elements define early and late cell cycle gene expression', *Oncotarget*, 8(58), pp. 97736–97748. Available at: https://doi.org/10.18632/oncotarget.10888.

Müller, R., Bleckmann, A. and Simon, R. (2008) 'The Receptor Kinase CORYNE of Arabidopsis Transmits the Stem Cell–Limiting Signal CLAVATA3 Independently of CLAVATA1', *The Plant Cell*, 20(4), pp. 934–946. Available at: https://doi.org/10.1105/tpc.107.057547.

Musa, J. *et al.* (2017) 'MYBL2 (B-Myb): a central regulator of cell proliferation, cell survival and differentiation involved in tumorigenesis', *Cell Death & Disease*, 8(6), pp. e2895–e2895. Available at: https://doi.org/10.1038/cddis.2017.244.

Nakajima, K. *et al.* (2001) 'Intercellular movement of the putative transcription factor SHR in root patterning', *Nature*, 413(6853), pp. 307–311. Available at: https://doi.org/10.1038/35095061.

Nieuwland, J., Menges, M. and Murray, J.A.H. (2007) 'The Plant Cyclins', in *Annual Plant Reviews Volume 32: Cell Cycle Control and Plant Development*. John Wiley & Sons, Ltd, pp. 31–61. Available at: https://doi.org/10.1002/9780470988923.ch2.

Ning, Y.-Q. *et al.* (2020) 'DREAM complex suppresses DNA methylation maintenance genes and precludes DNA hypermethylation', *Nature Plants*, 6(8), pp. 942–956. Available at: https://doi.org/10.1038/s41477-020-0710-7.

Ogawa, M. *et al.* (2008) 'Arabidopsis CLV3 Peptide Directly Binds CLV1 Ectodomain', *Science* [Preprint]. Available at: https://doi.org/10.1126/science.1150083.

O'Malley, R.C. *et al.* (2016) 'Cistrome and Epicistrome Features Shape the Regulatory DNA Landscape', *Cell*, 165(5), pp. 1280–1292. Available at: https://doi.org/10.1016/j.cell.2016.04.038.

Petricka, J.J., Winter, C.M. and Benfey, P.N. (2012) 'Control of Arabidopsis Root Development', *Annual Review of Plant Biology*, 63(1), pp. 563–590. Available at: https://doi.org/10.1146/annurev-arplant-042811-105501.

Poethig, S. (1989) ‘Genetic mosaics and cell lineage analysis in plants’, *Trends in genetics: TIG*, 5(8), pp. 273–277. Available at: https://doi.org/10.1016/0168-9525(89)90101-7.

Ryu, K.H. *et al.* (2019) ‘Single-Cell RNA Sequencing Resolves Molecular Relationships Among Individual Plant Cells’, *Plant Physiology*, 179(4), pp. 1444–1456. Available at: https://doi.org/10.1104/pp.18.01482.

Sadasivam, S. and DeCaprio, J.A. (2013a) ‘The DREAM complex: master coordinator of cell cycle-dependent gene expression’, *Nature Reviews Cancer*, 13(8), pp. 585–595. Available at: https://doi.org/10.1038/nrc3556.

Sadasivam, S. and DeCaprio, J.A. (2013b) ‘The DREAM complex: master coordinator of cell cycle-dependent gene expression’, *Nature Reviews Cancer*, 13(8), pp. 585–595. Available at: https://doi.org/10.1038/nrc3556.

Sadasivam, S., Duan, S. and DeCaprio, J.A. (2012) ‘The MuvB complex sequentially recruits B-Myb and FoxM1 to promote mitotic gene expression’, *Genes & Development*, 26(5), pp. 474–489. Available at: https://doi.org/10.1101/gad.181933.111.

Sarkar, A.K. *et al.* (2007) ‘Conserved factors regulate signalling in Arabidopsis thaliana shoot and root stem cell organizers’, *Nature*, 446(7137), pp. 811–814. Available at: https://doi.org/10.1038/nature05703.

Satija, R. *et al.* (2015) ‘Spatial reconstruction of single-cell gene expression data’, *Nature Biotechnology*, 33(5), pp. 495–502. Available at: https://doi.org/10.1038/nbt.3192.

Schafer, K.A. (1998) ‘The Cell Cycle: A Review’, *Veterinary Pathology*, 35(6), pp. 461–478. Available at: https://doi.org/10.1177/030098589803500601.

Schmit, F. *et al.* (2007) ‘LINC, a Human Complex That is Related to pRB-Containing Complexes in Invertebrates Regulates the Expression of G2/M Genes’, *Cell Cycle*, 6(15), pp. 1903–1913. Available at: https://doi.org/10.4161/cc.6.15.4512.

Schmit, F., Cremer, S. and Gaubatz, S. (2009) ‘LIN54 is an essential core subunit of the DREAM/LINC complex that binds to the cdc2 promoter in a sequence-specific manner’, *The FEBS Journal*, 276(19), pp. 5703–5716. Available at: https://doi.org/10.1111/j.1742-4658.2009.07261.x.

Schoof, H. *et al.* (2000) ‘The Stem Cell Population of Arabidopsis Shoot Meristems Is Maintained by a Regulatory Loop between the CLAVATA and WUSCHEL Genes’, *Cell*, 100(6), pp. 635–644. Available at: https://doi.org/10.1016/S0092-8674(00)80700-X.

Shahan, R. *et al.* (2022) 'A single-cell Arabidopsis root atlas reveals developmental trajectories in wild-type and cell identity mutants', *Developmental Cell*, 57(4), pp. 543-560.e9. Available at: https://doi.org/10.1016/j.devcel.2022.01.008.

Shaw, R., Tian, X. and Xu, J. (2021) 'Single-Cell Transcriptome Analysis in Plants: Advances and Challenges', *Molecular Plant*, 14(1), pp. 115–126. Available at: https://doi.org/10.1016/j.molp.2020.10.012.

Sijacic, P., Wang, W. and Liu, Z. (2011) 'Recessive Antimorphic Alleles Overcome Functionally Redundant Loci to Reveal TSO1 Function in Arabidopsis Flowers and Meristems', *PLOS Genetics*, 7(11), p. e1002352. Available at: https://doi.org/10.1371/journal.pgen.1002352.

Simmons, A.R. *et al.* (2019) 'SOL1 and SOL2 regulate fate transition and cell divisions in the Arabidopsis stomatal lineage', *Development (Cambridge, England)*, 146(3), p. dev171066. Available at: https://doi.org/10.1242/dev.171066.

Song, J.Y. *et al.* (2000) 'Regulation of meristem organization and cell division by TSO1, an Arabidopsis gene with cysteine-rich repeats', *Development (Cambridge, England)*, 127(10), pp. 2207–2217.

Soni, R. *et al.* (1995) 'A family of cyclin D homologs from plants differentially controlled by growth regulators and containing the conserved retinoblastoma protein interaction motif.', *The Plant Cell*, 7(1), pp. 85–103. Available at: https://doi.org/10.1105/tpc.7.1.85.

Stahl, Y. *et al.* (2009) 'A signaling module controlling the stem cell niche in Arabidopsis root meristems', *Current biology: CB*, 19(11), pp. 909–914. Available at: https://doi.org/10.1016/j.cub.2009.03.060.

Stepanova, A.N. *et al.* (2005) 'A Link between ethylene and auxin uncovered by the characterization of two root-specific ethylene-insensitive mutants in Arabidopsis', *The Plant Cell*, 17(8), pp. 2230–2242. Available at: https://doi.org/10.1105/tpc.105.033365.

Stepanova, A.N. *et al.* (2008) 'TAA1-Mediated Auxin Biosynthesis Is Essential for Hormone Crosstalk and Plant Development', *Cell*, 133(1), pp. 177–191. Available at: https://doi.org/10.1016/j.cell.2008.01.047.

Takahashi, I. *et al.* (2010) 'Two Arabidopsis cyclin A3s possess G1 cyclin-like features', *Plant Cell Reports*, 29(4), pp. 307–315. Available at: https://doi.org/10.1007/s00299-010-0817-9.

Tang, G. *et al.* (2003) 'A biochemical framework for RNA silencing in plants', *Genes & Development*, 17(1), pp. 49–63. Available at: https://doi.org/10.1101/gad.1048103.

Tank, J.G. and Thaker, V.S. (2011) 'Cyclin dependent kinases and their role in regulation of plant cell cycle', *Biologia Plantarum*, 55(2), p. 201. Available at: https://doi.org/10.1007/s10535-011-0031-9.

Taylor-Teeples, M. *et al.* (2015) 'An Arabidopsis gene regulatory network for secondary cell wall synthesis', *Nature*, 517(7536), pp. 571–575. Available at: https://doi.org/10.1038/nature14099.

Thimann, K.V. (1936) 'Auxins and the Growth of Roots', *American Journal of Botany*, 23(8), pp. 561–569. Available at: https://doi.org/10.2307/2436087.

Truman, A.W. *et al.* (2012) 'Cell Cycle: Regulation by Cyclins', in *eLS*. John Wiley & Sons, Ltd. Available at: https://doi.org/10.1002/9780470015902.a0001364.pub3.

Van Leene, J. *et al.* (2010) 'Targeted interactomics reveals a complex core cell cycle machinery in Arabidopsis thaliana', *Molecular Systems Biology*, 6, p. 397. Available at: https://doi.org/10.1038/msb.2010.53.

Wachsman, G. *et al.* (2017) 'A SIMPLE Pipeline for Mapping Point Mutations', *Plant Physiology*, 174(3), pp. 1307–1313. Available at: https://doi.org/10.1104/pp.17.00415.

Wang, W. *et al.* (2018) 'Arabidopsis TSO1 and MYB3R1 form a regulatory module to coordinate cell proliferation with differentiation in shoot and root', *Proceedings of the National Academy of Sciences of the United States of America*, 115(13), pp. E3045–E3054. Available at: https://doi.org/10.1073/pnas.1715903115.

Wang, Z.-P. *et al.* (2015) 'Egg cell-specific promoter-controlled CRISPR/Cas9 efficiently generates homozygous mutants for multiple target genes in Arabidopsis in a single generation', *Genome Biology*, 16, p. 144. Available at: https://doi.org/10.1186/s13059-015-0715-0.

Willems, A. *et al.* (2020) 'The Cyclin CYCA3;4 Is a Postprophase Target of the APC/CCCS52A2 E3-Ligase Controlling Formative Cell Divisions in Arabidopsis', *The Plant Cell*, 32(9), pp. 2979–2996. Available at: https://doi.org/10.1105/tpc.20.00208.

Wu, N. *et al.* (2017) 'A mouse model of MYCN-driven retinoblastoma reveals MYCN-independent tumor reemergence', *The Journal of Clinical Investigation*, 127(3), pp. 888–898. Available at: https://doi.org/10.1172/JCI88508.

Wysocka-Diller, J. *et al.* (2000) 'Molecular analysis of SCARECROW function reveals a radial patterning mechanism common to root and shoot.', *Development* [Preprint].

Xie, Y. *et al.* (2020) 'Single-Cell RNA Sequencing Efficiently Predicts Transcription Factor Targets in Plants', *Frontiers in Plant Science*, 11. Available at:

https://www.frontiersin.org/article/10.3389/fpls.2020.603302 (Accessed: 9 March 2022).

Yadav, R.K. *et al.* (2011) 'WUSCHEL protein movement mediates stem cell homeostasis in the Arabidopsis shoot apex', *Genes & Development*, 25(19), pp. 2025–2030. Available at: https://doi.org/10.1101/gad.17258511.

Yang, W. *et al.* (2021) 'Molecular mechanism of cytokinin-activated cell division in Arabidopsis', *Science (New York, N.Y.)*, 371(6536), pp. 1350–1355. Available at: https://doi.org/10.1126/science.abe2305.

Yu, Y. *et al.* (2003) 'The Tobacco A-Type Cyclin, Nicta;CYCA3;2, at the Nexus of Cell Division and Differentiation', *The Plant Cell*, 15(12), pp. 2763–2777. Available at: https://doi.org/10.1105/tpc.015990.

Zhan, J. *et al.* (2018) 'Opaque-2 Regulates a Complex Gene Network Associated with Cell Differentiation and Storage Functions of Maize Endosperm', *The Plant Cell*, 30(10), pp. 2425–2446. Available at: https://doi.org/10.1105/tpc.18.00392.

Zhang, F., May, A. and Irish, V.F. (2017) 'Type-B ARABIDOPSIS RESPONSE REGULATORs Directly Activate WUSCHEL', *Trends in Plant Science*, 22(10), pp. 815–817. Available at: https://doi.org/10.1016/j.tplants.2017.08.007.

Zhang, T.-Q., Chen, Y. and Wang, J.-W. (2021) 'A single-cell analysis of the Arabidopsis vegetative shoot apex', *Developmental Cell*, 56(7), pp. 1056-1074.e8. Available at: https://doi.org/10.1016/j.devcel.2021.02.021.

Zheng, G.X.Y. *et al.* (2017) 'Massively parallel digital transcriptional profiling of single cells', *Nature Communications*, 8(1), p. 14049. Available at: https://doi.org/10.1038/ncomms14049.

Zhong, R. and Ye, Z.-H. (2004) 'amphivasal vascular bundle 1, a Gain-of-Function Mutation of the IFL1/REV Gene, Is Associated with Alterations in the Polarity of Leaves, Stems and Carpels', *Plant and Cell Physiology*, 45(4), pp. 369–385. Available at: https://doi.org/10.1093/pcp/pch051.

Zhou, G.-K. *et al.* (2007) 'Overexpression of miR165 Affects Apical Meristem Formation, Organ Polarity Establishment and Vascular Development in Arabidopsis', *Plant and Cell Physiology*, 48(3), pp. 391–404. Available at: https://doi.org/10.1093/pcp/pcm008.

Zhou, J. *et al.* (2021) 'Gibberellin and auxin signaling genes RGA1 and ARF8 repress accessory fruit initiation in diploid strawberry', *Plant Physiology*, 185(3), pp. 1059–1075. Available at: https://doi.org/10.1093/plphys/kiaa087.